Li X, Yang HY, Giachelli CM. 2006. Role of the sodium-dependent phosphate cotransporter, Pit-1, in vascular smooth muscle cell calcification. Circ Res 98:905–912.

Liu S, Tang W, Zhou J, Stubbs JR, Luo Q, Pi M, Quarles LD. 2006. Fibroblast growth factor 23 is a counter-regulatory phosphaturic hormone for vitamin D. J Am Soc Nephrol 17:1305–1315.

Liu S, Vierthaler L, Tang W, Zhou J, Quarles LD. 2008. FGFR3 and FGFR4 do not mediate renal effects of FGF23. J Am Soc Nephrol 19:2342–2350.

Mizobuchi M, Ogata H, Hatamura I, Koiwa F, Saji F, Shiizaki K, Negi S, Kinugasa E, Ooshima A, Koshikawa S, Akizawa T. 2006. Up-regulation of Cbfa1 and Pit-1 in calcified artery of uraemic rats with severe hyperphosphataemia and secondary hyperparathyroidism. Nephrol Dial Transplant 21:911–916.

Nishida Y, Taketani Y, Yamanaka-Okumura H, Imamura F, Taniguchi A, Sato T, Shuto E, Nashiki K, Arai H, Yamamoto H, Takeda E. 2006. Acute effect of oral phosphate loading on serum fibroblast growth factor 23 levels in healthy men. Kidney Int 70:2141–2147.

Nowik M, Picard N, Stange G, Capuano P, Tenenhouse HS, Biber J, Murer H, Wagner CA. 2008. Renal phosphaturia during metabolic acidosis revisited: Molecular mechanisms for decreased renal phosphate reabsorption. Pflugers Arch 457:539–549.

Pande S, Ritter CS, Rothstein M, Wiesen K, Vassiliadis J, Kumar R, Schiavi SC, Slatapolsky E, Brown AJ. 2006. FGF-23 and sFRP-4 in chronic kidney disease and post-renal transplantation. Nephron Physiol 104:23–32.

Perwad F, Azam N, Zhang MY, Yamashita T, Tenenhouse HS, Portale AA. 2005. Dietary and serum phosphorus regulate fibroblast growth factor 23 expression and 1,25-dihydroxyvitamin D metabolism in mice. Endocrinology 146:5358–5364.

Quarles LD. 2008. Endocrine functions of bone in mineral metabolism regulation. J Clin Invest 118:3820–3828.

Saito H, Kusano K, Kinosaki M, Ito H, Hirata M, Segawa H, Miyamoto K, Fukushima N. 2003. Human fibroblast growth factor-23 mutants suppress Na+-dependent phosphate co-transport activity and 1alpha,25-dihydroxyvitamin D3 production. J Biol Chem 278:2206–2211.

Segawa H, Kawakami E, Kaneko I, Kuwahata M, Ito M, Kusano K, Saito H, Fukushima N, Miyamoto K. 2003. Effect of hydrolysis-resistant FGF23-R179Q on dietary phosphate regulation of the renal type-II Na/Pi transporter. Pflugers Arch 446:585–592.

Shimada T, Mizutani S, Muto T, Yoneya T, Hino R, Takeda S, Takeuchi Y, Fujita T, Fukumoto S, Yamashita T. 2001. Cloning and characterization of FGF23 as a causative factor of tumor-induced osteomalacia. Proc Natl Acad Sci USA 98:6500–6505.

Shimada T, Hasegawa H, Yamazaki Y, Muto T, Hino R, Takeuchi Y, Fujita T, Nakahara K, Fukumoto S, Yamashita T. 2004a. FGF-23 is a potent regulator of vitamin D metabolism and phosphate homeostasis. J Bone Miner Res 19: 429–435.

Shimada T, Kakitani M, Yamazaki Y, Hasegawa H, Takeuchi Y, Fujita T, Fukumoto S, Tomizuka K, Yamashita T. 2004b. Targeted ablation of Fgf23 demonstrates an essential physiological role of FGF23 in phosphate and vitamin D metabolism. J Clin Invest 113:561–568.

Urakawa I, Yamazaki Y, Shimada T, Iijima K, Hasegawa H, Okawa K, Fujita T, Fukumoto S, Yamashita T. 2006. Klotho converts canonical FGF receptor into a specific receptor for FGF23. Nature 444:770–774.

Villa-Bellosta R, Ravera S, Sorribas V, Stange G, Levi M, Murer H, Biber J, Forster IC. 2009. The Na+–Pi cotransporter PiT-2 (SLC20A2) is expressed in the apical membrane of rat renal proximal tubules and regulated by dietary Pi. Am J Physiol Renal Physiol 296:F691–F699.

Virkki LV, Biber J, Murer H, Forster IC. 2007. Phosphate transporters: A tale of two solute carrier families. Am J Physiol Renal Physiol 293:F643–F654.

Weber TJ, Liu S, Indridason OS, Quarles LD. 2003. Serum FGF23 levels in normal and disordered phosphorus homeostasis. J Bone Miner Res 18:1227–1234.

Westerberg PA, Linde T, Wikstrom B, Ljunggren O, Stridsberg M, Larsson TE. 2007. Regulation of fibroblast growth factor-23 in chronic kidney disease. Nephrol Dial Transplant 22:3202–3207.

ORIGINAL ARTICLE

JBMR

Prolonged Survival and Phenotypic Correction of *Akp2*$^{-/-}$ Hypophosphatasia Mice by Lentiviral Gene Therapy

Seiko Yamamoto,[1,2] Hideo Orimo,[1] Tae Matsumoto,[1] Osamu Iijima,[1] Sonoko Narisawa,[3] Takahide Maeda,[2] José Luis Millán,[3] and Takashi Shimada[1]

[1]Department of Biochemistry and Molecular Biology, Nippon Medical School, Tokyo, Japan
[2]Department of Pediatric Dentistry, Nihon University Graduate School of Dentistry at Matsudo, Matsudo, Japan
[3]Sanford-Burnham Medical Research Institute, La Jolla, CA, USA

ABSTRACT

Hypophosphatasia (HPP) is an inherited systemic skeletal disease caused by mutations in the gene encoding the tissue-nonspecific alkaline phosphatase (*TNALP*) isozyme. The clinical severity of HPP varies widely, with symptoms including rickets and osteomalacia. *TNALP* knockout (*Akp2*$^{-/-}$) mice phenotypically mimic the severe infantile form of HPP; that is, *TNALP*-deficient mice are born with a normal appearance but die by 20 days of age owing to growth failure, hypomineralization, and epileptic seizures. In this study, a lentiviral vector expressing a bone-targeted form of *TNALP* was injected into the jugular vein of newborn *Akp2*$^{-/-}$ mice. We found that alkaline phosphatase activity in the plasma of treated *Akp2*$^{-/-}$ mice increased and remained at high levels throughout the life of the animals. The treated *Akp2*$^{-/-}$ mice survived for more than 10 months and demonstrated normal physical activity and a healthy appearance. Epileptic seizures were completely inhibited in the treated *Akp2*$^{-/-}$ mice, and X-ray examination of the skeleton showed that mineralization was significantly improved by the gene therapy. These results show that severe infantile HPP in *TNALP* knockout mice can be treated with a single injection of lentiviral vector during the neonatal period. © 2011 American Society for Bone and Mineral Research.

KEY WORDS: ALKALINE PHOSPHATASE; LENTIVIRAL VECTOR; ENZYME REPLACEMENT; EPILEPSY; CALCIFICATION

Introduction

Hypophosphatasia (HPP) is an inherited skeletal disease caused by mutations in the gene encoding the tissue-nonspecific alkaline phosphatase (*TNALP*) isozyme.[1] The symptoms of HPP include hypomineralization that causes rickets in infants and children and osteomalacia in adults.[2,3] The clinical severity of HPP varies widely from a lethal perinatal form to mild odontohypophosphatasia that manifests only dental abnormalities.[4] In the infantile form, postnatal development appears to proceed normally before the onset of failure to thrive and the associated development of rickets before 6 months of age. Severe infantile HPP is often fatal.[3]

TNALP is an ectoenzyme that is attached to the outer plasma membrane via a glycosylphosphatidylinositol (GPI) anchor.[5,6] Absence of TNALP activity results in extracellular accumulation of natural substrates such as inorganic pyrophosphate (PP_i),[7,8] pyridoxal 5′-phosphate (PLP),[9,10] and phosphoethanolamine (PEA).[11] Since high concentrations of PP_i result in a strong inhibition of hydroxylapatite crystal growth, normal mineralization of the systemic bones and teeth is impaired in HPP patients.[8,12] Pyridoxine-responsive seizures are also observed in some severe cases. Enzyme-replacement therapy using various types of alkaline phosphatase[13–17] and cell therapy using bone marrow cells[18,19] and mesenchymal cells[20] have been reported with no or very limited clinical benefit.

TNALP knockout mice have been established in two independent laboratories.[21,22] These mice are born with a normal appearance but, owing to deficient degradation of PP_i and abnormal metabolism of PLP, develop rickets and die by 20 days of age as a result of severe skeletal hypomineralization and epileptic seizures and represent an appropriate model of the infantile form of HPP.[23,24] Recently, Millán and colleagues[25] treated *TNALP* knockout mice with a daily subcutaneous injection of a bone-targeted form of TNALP in which a bone-targeting deca-aspartate sequence was linked to the C-terminal end of soluble TNALP.[26,27] Based on those data, clinical trials of enzyme-replacement therapy with bone-targeted TNALP in

Received in original form December 31, 2009; revised form June 5, 2010; accepted July 22, 2010. Published online August 4, 2010.
Address correspondence to: Takashi Shimada, MD, PhD, Department of Biochemistry and Molecular Biology, Nippon Medical School, 1-1-5 Sendagi, Bunkyo-ku, Tokyo 113-8602, Japan. E-mail: tshimada@nms.ac.jp
Journal of Bone and Mineral Research, Vol. 26, No. 1, January 2011, pp 135–142
DOI: 10.1002/jbmr.201

patients with adult and infantile HPP have been initiated.[28] A limitation of enzyme-replacement therapy for HPP is the restricted half-life of the TNALP protein in patients' fluids and tissues, which necessitates repeated administration of large amounts of the enzyme for long-term correction.

In this study, we examined viral vector–mediated gene therapy of HPP. We found that a single injection of lentiviral vector expressing bone-targeted TNALP into neonatal HPP mice resulted in long-term high levels of ALP in the serum and long-term phenotypic correction in HPP mice. We conclude that gene therapy may prove to be an important option for the treatment of human HPP.

Materials and Methods

Plasmid construction

To create *TNALP-D10* cDNA coding for TNALP lacking the GPI anchor sequence and containing 10 repeated aspartic acid (Asp) residues at its C-terminus, polymerase chain reaction (PCR) was performed using primers *TNALP-D10*-f (5′-GAA TTC ACC CAC GTC GAT TGC ATC TCT CTG GGC TCC AG) and *TNALP-D10*-r (5′-GAA TTC TCA GTC GTC ATC ATC ATC ATC GTC GTC ATC GTC GTC GCC TGC GGA GCT GGC AGG AGC ACA GTG-3′) with pcDNA3 *TNALP* cDNA plasmid as the template.[29] The PCR product then was digested with *Eco*RI and inserted into the pGEM T-easy vector (Promega Corporation, Madison, WI, USA). A second PCR was performed using primers *Eco*RI–*TNALP*-f (5′-TTT GAA TTC GCC ACC ATG ATT TCA CCA TTC TTA GTA C-3′) and *TNALP-D10-Not*I-r (5′-TTT GCG GCC GCT CAG TCG TCA TCA TCA TCA TCG). The orientation of each sequence then was confirmed.

The pHIV-TNALP-D10 plasmid was constructed by insertion of the *Eco*RI and *Not*I fragments containing the cDNA for *TNALP-D10* into pC1(–)3UTR-del, which is a newly constructed SJ1-based HIV-1 vector containing 0.25-kb insulators in the U3 and the murine stem cell virus (MSCV) long terminal repeat (LTR) as an internal promoter (Fig. 1*A*).[30]

Lentiviral vector preparation

Lentiviral vector was prepared by transient transfection in 293T cells, as described previously.[30] Vector preparation treated with Benzonase (50 μL/mL) for 1 hour at room temperature was filtrated by 0.45-μm membrane after adjustment of the pH to 8.0 with 1 N NaOH. Vector was concentrated using Acrodisc Units with Mustang Q Membranes (PALL Corporation, Ann Arbor, MI, USA).[31,32] The eluted solution containing lentiviral vector was ultracentrifuged with a 20% (w/v) sucrose underlay for purification, and the infectious vector particle (titer) was determined in HeLa cells. The titer was expressed as transducing units per milliliter (TU/mL).

Animal procedures and experiments

All animal experiments were preapproved by the Nippon Medical School Animal Ethics Committee. Wild-type (WT) $Akp2^{+/-}$ heterozygous (HET) and $Akp2^{-/-}$ knockout (HPP) mice were obtained by mating $Akp2^{+/-}$ heterozygous mice with mice of a mixed 129J × C57Bl/6J genetic background.[22] Lentiviral vector (5.0×10^7 TU/100 μL in PBS) was injected into the jugular vein of neonatal mice on days 1 through 3. Breeding HET pairs were fed modified Laboratory Rodent Diet 5001 (Purina Mills, St Louis, MO, USA)[35] composed of CMF laboratory feed (Oriental Yeast Co., Ltd., Tokyo, Japan) supplemented with 325 ppm pyridoxine/10 kg of feed.

ALP activity

Blood samples were collected from the tail vein or the orbital sinus. The level of ALP in the plasma was quantified using a colorimetric assay for ALP activity, as described previously.[36] ALP activity was determined using 10 mM *p*-nitrophenyl phosphate (Sigma-Aldrich, Steinheim, UK) as the substrate in 100 mM 2-amino-2-methyl-1,3-propanediol-HCl buffer containing 5 mM $MgCl_2$ (pH 10.0) at 37°C. ALP enzyme activity was described in units (U) defined as the amount of enzyme needed to catalyze production of 1 μmol of *p*-nitrophenol formed per minute. ALP activity in plasma was calculated as units per milliliter (U/mL).

Biodistribution of lentiviral vector

Mice were deepley anesthesized and perfused with 15 mL of PBS containing 150 U of heparin and 15 mL of PBS. The liver, spleen, kidney, lung, heart, and bone (femur) were harvested, and homogenates were made using the Percellys-24 bead-beating homogenizer according to the company's protocol (Bertin Technologies, Paris, France). Genomic DNA was extracted from tissue homogenates using the Gentra Puregene Kit (Qiagen Siences, Germantown, MD, USA) and was subjected to real-time PCR to estimate the distribution. The primer/probe sets FPLV2 (modified at one base to 5′-ACT TGA AAG CGA AAG GGA AAC-3′ owing to a difference in the HIV-1 strain), RPLV2 (5′-CAC CCA TCT CTC TCC TTC TAG CC-3′), and LV2 (5′-AGC TCT CTC GAC GCA GGA CTC GGC -3′) were used to detect the lentiviral vector provirus, as described previously.[33] TaqMan ribosomal RNA control reagents (Applied Biosystems, Branchburg, NJ, USA) were used to quantify the amount of genomic DNA. To estimate vector distribution, genomic DNA extracted from the bone marrow cells of BL/6 wild-type mice or genomic DNA spiked with plasmid DNA was used as a standard, and average copy number per diploid were determined.[34]

X-ray analysis

Digital microradiography images were obtained using a μFX-1000 (Fujifilm, Tokyo, Japan) and imaged with FLA-7000 (Fujifilm). The X-ray energy levels were 25 kV and 100 μA, and an exposure time of 90 seconds was used for 15-day-old mice, and 15 seconds was used for adult mice. We examined a minimum of three X-ray pictures from each group at given ages.

ALP activity staining

Bone samples were fixed in neutral buffered formalin for 24 hours at 4°C. Knuckle samples then were decalcified in 10% EDTA solution with rotation for 2 to 3 days at 4°C. For the azo-dye method, knuckles were embedded in optimal-cutting-temperature (OCT) compound (Tissue-Tek, SAKUSA Finetechnical, Tokyo, Japan) and sectioned using a Leica CM1950 cryostat. Thin sections (4 μm thick) were air-dried for 10 minutes, washed in

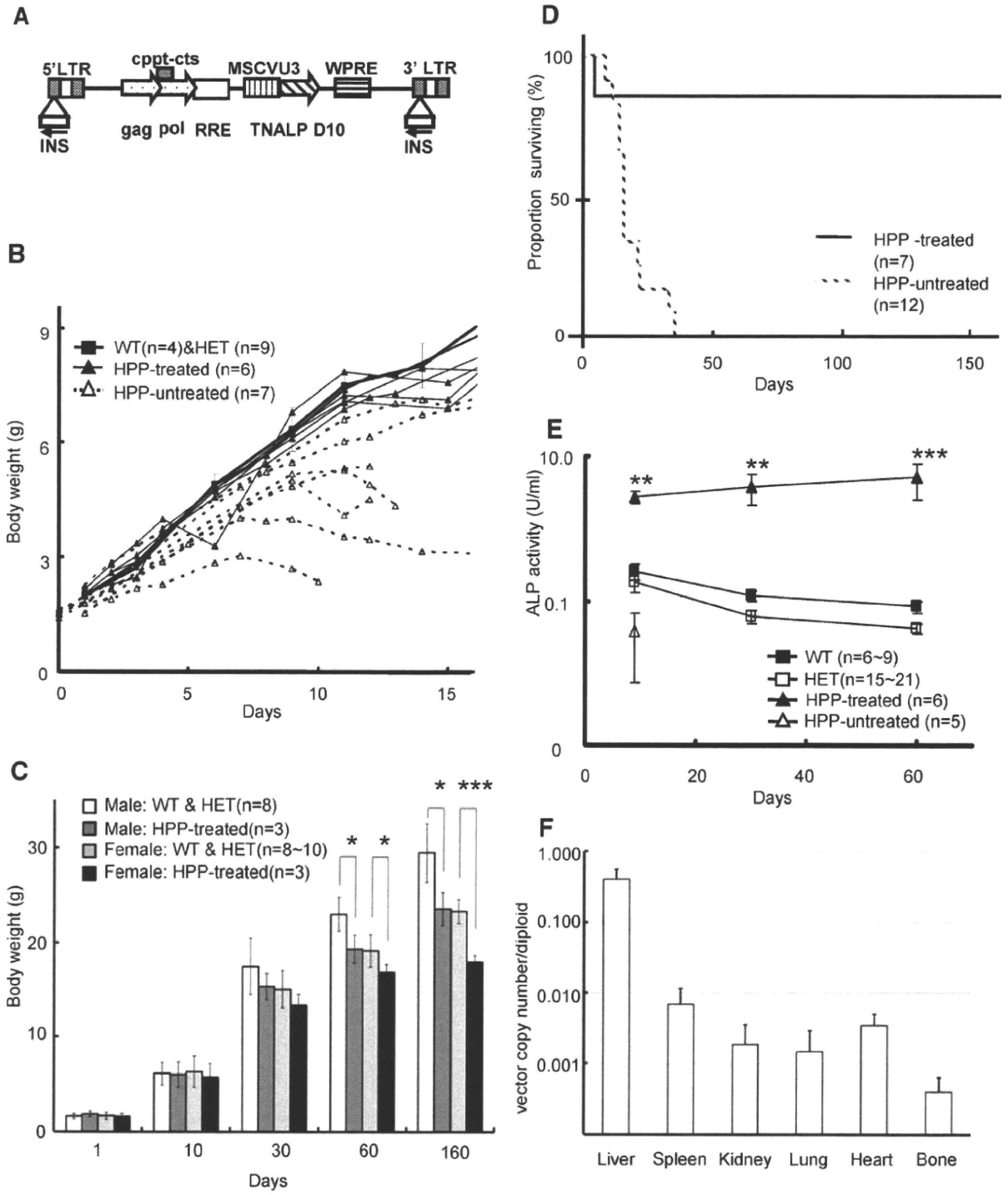

Fig. 1. Lentiviral-mediated gene therapy of *Akp2*$^{-/-}$ hypophosphatasic (HPP) mice. (*A*) Schematic diagram of HIV-TNALP-D10 lentiviral vector. LTR = long terminal repeat; MSCVU3 = U3 region of the LTR promoter of murine stem cell virus; WPRE = woodchuck hepatitis virus posttranscriptional regulatory element; INS = chicken β-globin hypersensitivity site 4 insulator; cppt-cts = central polypurine tract–central termination sequence; RRE = reverse responsive element. (*B*) Growth curves of untreated HPP mice ($n = 7$), treated HPP mice ($n = 6$), and WT ($n = 4$) and HET ($n = 9$) mice. The body weights of untreated HPP mice were recorded until spontaneous death. The weights of WT and HET (total $n = 13$) mice are presented as the average ± SD. (*C*) The comparison of average body weights of treated HPP mice (male, $n = 3$; female, $n = 3$) and WT/HET littermates (male, $n = 8$; female, $n = 8$ to 10). $^{*}p < .05$; $^{***}p < .001$. (*D*) The survival curves of treated ($n = 7$) and untreated ($n = 12$) HPP mice. (*E*) Concentration of plasma ALP in the treated ($n = 6$) and untreated ($n = 5$) HPP mice and HET ($n = 15$ to 21) and WT ($n = 6$-9) controls. $^{**}p < .01$ versus the WT group; $^{***}p < .001$ versus the WT group. (*F*) Distribution of lentiviral vector. The copy numbers of the vector genome in the organs was determined by qPCR with HIV-TNALP-D10 injected WT mice. Data are presented as mean ± SEM ($n = 4$).

PBS, and transferred to a solution of 50 mM $MgCl_2$ in 0.05 M Tris–maleic acid buffer (pH 7.4) for 30 minutes for the reactivation of ALP.[37] The sections then were incubated in a freshly prepared mixture of Naphthol AS-MX phosphate disodium salt (Sigma-Aldrich) and Fast Blue BB Salt (Sigma-Aldrich) as described previously.[38] Methyl green served as the counterstain.

Statistical analysis

Data are expressed as mean ± SD. Differences between two groups were tested for statistical significance using Student's *t* test. p values $< .05$ were considered statistically significant. Kaplan-Meier curves were produced and analyzed using SPSS for Windows, Version 14.0J (SPSS Japan, Tokyo, Japan).

Results

Growth and survival of *Akp2*$^{-/-}$ mice

The growth of the *Akp2*$^{+/-}$ HET mice appeared indistinguishable from that of the WT mice. The *Akp2*$^{-/-}$ HPP mice were born with a normal appearance and weight. However, HPP mice showed apparent growth failure and became progressively exhausted (Fig. 1*B*). Most of the HPP mice also developed spontaneous seizures with various clinical presentations, including tonic-clonic convulsions and abnormal running and vocalization. The mice usually died 1 to 2 days after the epileptic seizures began. The average life span of the HPP mice was 12.0 ± 4.4 days ($n = 13$). Pyridoxine supplementation of the food for the nursing mother delayed the onset of the epileptic attacks in the neonates and extended their survival to postnatal day 18.1 ± 7.6 ($n = 15$).

Lentiviral vector containing bone-targeted human *TNALP* cDNA (HIV-TNALP-D10) was injected into the jugular vein of the neonatal HPP mice on days 1 through 3 ($n = 6$). The weight and growth rates of the treated HPP mice were improved compared with the untreated HPP mice and were indistinguishable from those of their WT and HET littermates ($n = 13$; Fig. 1*B*). The long-term follow-up was done for 7 treated mice. Compared with untreated mice ($n = 12$), the life spans of treated mice ($n = 7$) were significantly extended up to at least 160 days of age, except that one treated animal died on day 6 from unknown causes (Fig. 1*D*). In the long survivors ($n = 6$), 3 were euthanized on day 160 for X-ray analysis, whereas the remaining 3 animals survived for more than 400 days with normal appearance and physical activity. Seizures were not observed in the treated mice throughout the experimental period. The average body weights of treated HPP ($n = 6$) and WT/HET ($n = 13$ to 18) were compared on days 1, 10, 30, 60, and 160 (Fig. 1*C*). The body weights differed between male and female mice after 60 days. In either gender, the slight but significant growth retardation was detected in treated HPP mice on days 60 and 160.

Lentivirus-mediated expression of ALP

At 10 to 12 days after birth, ALP activity in the plasma of WT and HET mice was 0.25 ± 0.07 U/mL ($n = 9$) and 0.16 ± 0.05 U/mL ($n = 21$), respectively, whereas that of the HPP mice was less than 0.1 U/mL ($n = 5$; Fig. 1*E*). A single injection of HIV-TNALP-D10 into the neonatal HPP mice ($n = 6$) on days 1 through 3 resulted in extremely high levels of plasma ALP (2.67 ± 0.56 U/mL). The plasma ALP activity in the WT and HET mice decreased slowly with aging, whereas the lentivirus-mediated expression of ALP remained stable, and the high levels of ALP activity persisted for at least 6 months. At 60 days of age, the average ALP activity in the treated HPP mice was 73-fold higher than that of the WT mice (5.14 ± 2.66 versus 0.07 ± 0.02).

Biodistribution of lentiviral vector was determined using quantitative PCR (qPCR) on genomic DNA isolated from the injected WT littermate mice 14 days after injection (Fig. 1*F*). The highest copy number of integrated vector was detected in liver samples (0.40 copy/diploid). Low levels of lentiviral integration also were observed in the spleen and the heart. Transduction of the bone tissue, including bone marrow cells, was very low (<0.001 copy/diploid).

Radiographic analysis

Since radiographic changes in the HPP mice were not apparent during the first 8 days of life, we examined X-ray images of the feet and legs of mice at approximately 20 days after birth. The severity of the mineralization defects in the untreated HPP mice was found to be highly variable. In the most severely affected cases, the metacarpal and digital bones were significantly shorter than those of the WT mice, and their epiphyses were not detected. In addition, some of the carpal bones were absent. We also observed the absence of secondary ossification centers in the feet (Fig. 2). The most severe phenotype was observed in approximately 10% of the *Akp2*$^{-/-}$ homozygous neonates, and these mice usually died by 10 days of age. In the milder cases, the epiphyses and all the digital bones were significantly mineralized, even though the HPP mice were smaller than the HET and WT mice. Heterogeneous radiographic changes between these two extreme phenotypes were observed in the untreated HPP mice.

X-ray images of treated HPP mice showed that mineralization was accelerated following lentivirus-mediated expression of TNALP-D10. Secondary ossification centers were detected in the feet of all treated animals at 15 days of age, although the intensity of the mineralization was variable. Ossification of the carpal bones also was improved. All the untreated HPP mice died, with an average survival of 18.1 days. No differences in skeletal structure and mineralization were observed between the long survivors after treatment and the WT mice at 100 days of age. These results indicate that mineralization defects in HPP mice can be corrected efficiently by gene therapy.

Histochemical examination of the bone

The proximal tibias were analyzed histochemically for ALP activity using the azo-dye technique with methyl green counterstaining (Fig. 3). Strong ALP activity was detected in both the bone and hypertrophic cartilage zones of the WT mice (Fig. 3*A*), whereas no ALP signal was observed in the epiphysis of the HPP mice (Fig. 3*B*). After treatment with lentiviral vector, faint ALP staining was observed on the surface of the endosteal bone (Fig. 3*C*, *D*).

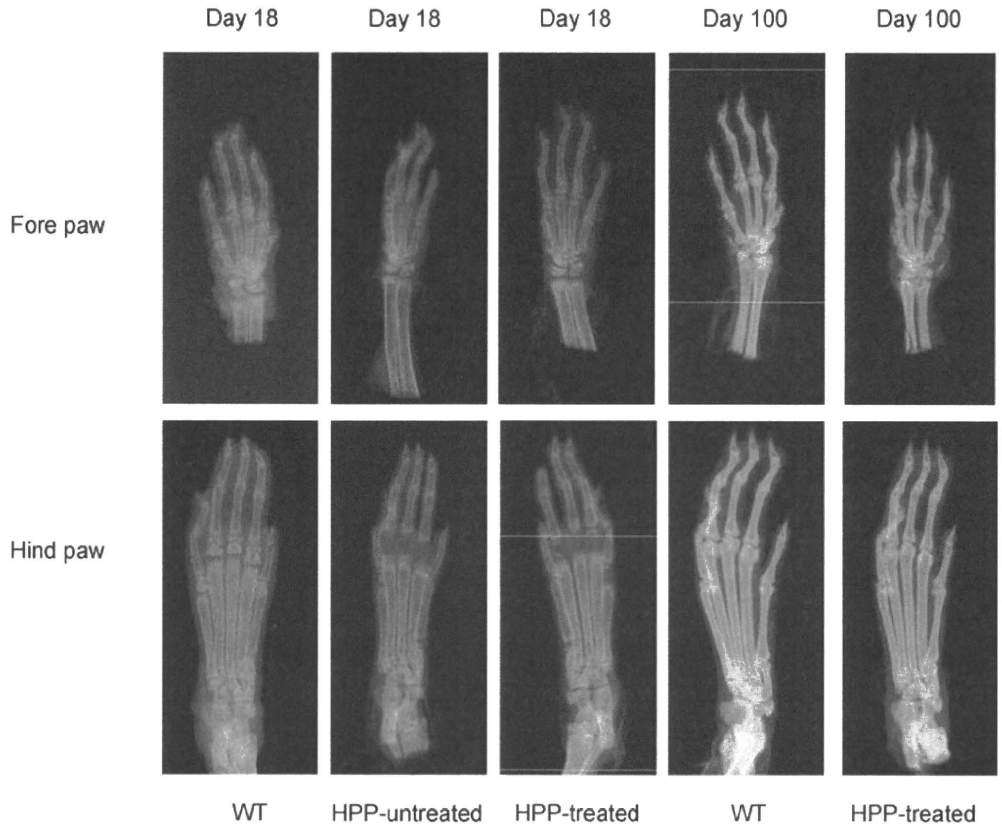

Fig. 2. X-ray images of the feet. Secondary ossification centers in the hind paws were absent in untreated HPP mice but were detectable in the treated mice at 18 days after birth. No differences in skeletal mineralization were observed between treated long survivors and WT mice at 100 days of age.

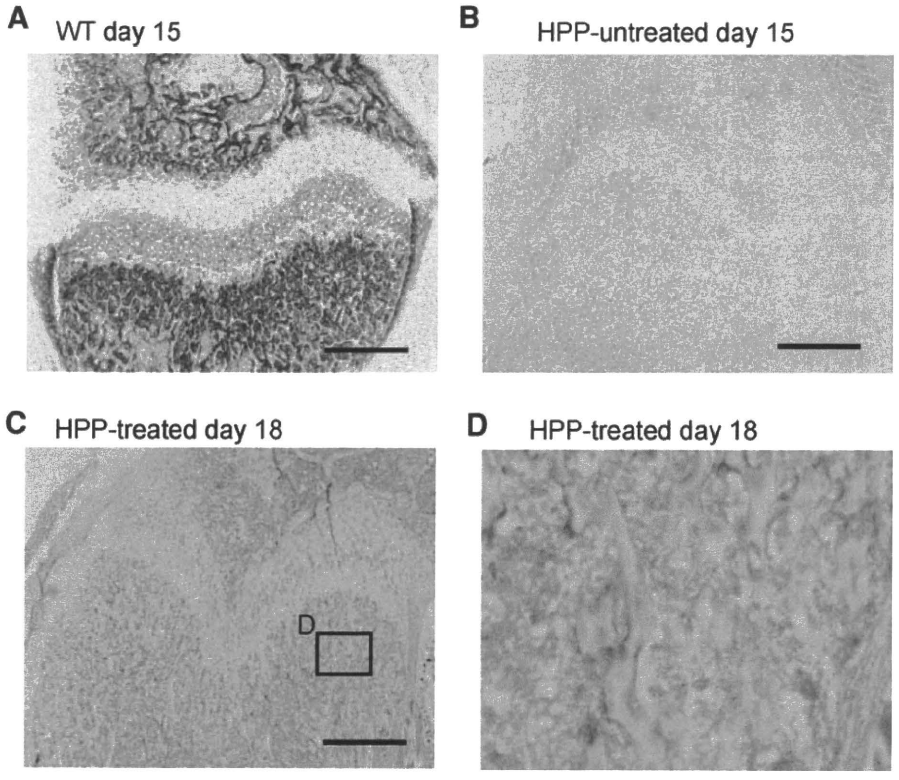

Fig. 3. Histochemical staining of ALP activity in the tibias. ALP activity was detected in WT (*A*) but not HPP mice (*B*) at 15 days after birth. Following treatment with lentiviral vector, (*C*) ALP activity was detected on the surface of the endosteal bone at 18 days after birth. (*D*) Magnified image of the square in panel *C*. Bars = 1 mm.

Discussion

TNALP is an ectoenzyme that is known to be particularly abundant on the cell surfaces of osteoblasts and hypertrophic chondrocytes, including their shed matrix vesicles.[6,39] Since ALP functions on the exterior of the cell, enzyme replacement following repeated administration of soluble ALP has been hypothesized as a potential approach to treat ALP deficiencies. However, the outcomes of previous clinical trials of enzyme-replacement therapy have proven disappointing. Intravenous infusions of ALP-rich serum from patients with Paget disease[13,14] and purified soluble ALP from human liver[16] and placenta[17] have shown no significant clinical benefits in patients with HPP. Recently, Millán and colleagues[25] demonstrated that daily injections of high-dose bone-targeted TNALP significantly extended the lifespan and corrected the abnormal phenotypes of HPP mice, suggesting that HPP could be treated by enzyme replacement if sufficient amounts of TNALP were able to reach the sites of skeletal mineralization. Based on these data, new clinical trials involving enzyme-replacement therapy for HPP patients have been initiated.[28]

A general problem of enzyme-replacement therapy is the short half-life of the administered protein in patients. A pharmacokinetic study showed that the half-life of bone-targeted TNALP is 34 hours in the plasma of adult mice, but in bone tissue the half-life is extended to more than 300 hours.[25] Nevertheless, repeated administration of large amounts of the enzyme is required for long-term correction. In the initial clinical trials, HPP patients received subcutaneous injections of bone-targeted TNALP three times weekly.[28] The preparation of adequate amounts of clinical-grade purified enzyme is a limitation, and repeated injection is highly invasive and not optimal for small children. In this study we demonstrated that a single injection of lentiviral vector resulted in sustained expression of ALP and phenotypic correction in HPP neonatal mice. As such, viral vector–mediated enzyme replacement may prove to be more practical than classic enzyme replacement by repeated injection.

One of the concerns of gene therapy is the safety of the viral vector. We used an HIV-1-based lentiviral vector in this study.[30] Lentivirus-mediated gene transfer has proven to be effective for long-term expression of transgenes in nondividing cells. Although the pathogenicity of HIV-1 was almost negligible in the current modified version of lentiviral vector, insertional mutagenesis is still a major concern for all integrating vectors.[40] To minimize the possibility of protooncogene activation, our novel self-inactivating lentiviral vector contains the insulator element from the chicken β-globin locus.[30] So far, lymphoproliferative complications owing to insertional mutagenesis have been detected in ex vivo hematopoietic stem cell gene therapy only. For the treatment of HPP, lentiviral vector was injected directly into the circulation of neonatal mice. After this in vivo systemic gene therapy, the lentiviral sequence was detected in the liver, lung, and heart. The oncogenicity of the integrated lentiviral vector in these differentiated tissues requires further examination in a long-term follow-up study.

We also found that the epileptic seizures were completely inhibited and the lifespan was significantly extended in the treated HPP mice. Without treatment, HPP mice died by 20 days of age.[22,35] The major cause of death in the untreated HPP mice was apnea, most likely resulting from their severe epileptic convulsions.[21] Pyridoxine-responsive seizures in HPP patients and HPP model mice are thought to be caused by reduced levels of the inhibitory neurotransmitter γ-aminobutyric acid (GABA) in the brain.[21,35] PLP is an essential cofactor of glutamate decarboxylase, which is responsible for the synthesis of GABA.[41] Diminished hydrolysis of extracellular PLP in HPP causes decreased intracellular pyridoxal levels in cells. This results in a reduction in the rephosphorylation of pyridoxal to PLP, and thus biosynthesis of GABA within the brain cells is reduced.[10] The seizure phenotype can be rescued in part by administration of pyridoxal.[23] We demonstrated that epileptic seizures were efficiently inhibited by either systemic infusion of TNALP[25] or viral vector–mediated expression of TNALP, suggesting that the defective metabolism of PLP in the brain could be corrected by replacement of soluble TNALP.

Although epileptic seizures are observed in some severely affected patients, the major clinical complications in human HPP patients are directly related to defective skeletal mineralization.[3] Patients with severe infantile HPP usually die from respiratory failure caused by skeletal diseases in the chest, such as flail chest, rachitic deformity, and rib fractures.[3] Compared with severe infantile HPP in human patients, bone defects in our mouse model are relatively mild. The *Akp2*$^{-/-}$ HPP mice were born with a normal appearance and bone mineral deposition. Hypomineralization becomes apparent after around 10 days of age, although the severity of mineralization defects varies widely.[22] Lentivirus-mediated expression of bone-targeted ALP efficiently prevents the progressive skeletal demineralization, as well as the lethal epilepsy.

Since enzyme replacement also was effective,[25] the major mechanism of successful gene therapy for HPP mice seems to be due to continuous supply of bone-targeted TNALP from the vector-infected liver to the circulation. Another possibility is that osteoblasts and chondrocytes may be directly transduced with lentiviral vector. However, since the copy number of integrated vector in the whole bone tissue was very low, the ALP staining in treated mice is mainly due to the circulating TNALP-D10 in the bone matrix. The contribution of in situ expression of TNALP in bone cells to bone mineralization is not likely to be significant.

A major physiologic role for TNALP has been shown to be the restriction of the extracellular pool of PP_i, which is a strong inhibitor for mineralization.[24,39] Localization of TNALP to the skeleton should be important for the treatment of HPP. TNALP with a repetitive C-terminal extension of 10 Asp was shown to display high affinity for bone tissue both in vitro[26] and in vivo.[25] The use of the bone-targeted TNALP construct in a clinical setting is currently under investigation in clinical trials.[28]

The efficacy of gene therapy to correct hypomineralization was evaluated by radiographic examination. The major problem is that the severity of the mineralization defects in untreated infantile *Akp2*$^{-/-}$ mice is highly variable. In addition, X-rays of infantile mice could be taken only after euthanization. The time course of mineralization in a single animal could not be

examined under the condition used. Further studies using more reliable histomorphometric and micro-computed tomographic (μCT) techniques may be required to optimize the gene therapy protocol to rescue the skeletal phenotype.

In conclusion, we found that severe infantile HPP in *TNALP* knockout mice can be treated with a single injection of lentiviral vector during the neonatal period. Lentiviral-mediated gene therapy may prove to be an important option in the treatment of human hypophosphatasia.

Disclosures

JLM is a consultant for Enobia Pharma, Inc. All the other authors state that they have no conflicts of interest.

Acknowledgments

We thank H Hanawa for technical support and Y Hirai for assistance in preparation of the manuscript. This work was supported in part by grants from the Ministry of Health, Labor and Welfare of Japan (HO and TS), Grant DE12889 from the National Institutes of Health, USA (JLM), and a grant from the Thrasher Research Fund (JLM).

References

1. Rathbun JC. Hypophosphatasia: a new developmental anomaly. Am J Dis Child. 1948;75:822–831.
2. Whyte MP. Hypophosphatasia and the role of alkaline phosphatase in skeletal mineralization. Endocr Rev. 1994;15:439–461.
3. Whyte MP. Hypophosphataia,. In: Scriver CR, Beaudet AL, Sly WS, Valle D, Childs B, Kinzler KW, eds. *The Metabolic and Molecular Bases of Inherited Deseases* 8th ed, Vol IV. New York: McGraw-Hill, 2002: 5319–5329.
4. Pimstone B, Eisenberg E, Silverman S. Hypophosphatasia: genetic and dental studies. Ann Intern Med. 1966;65:722–7229.
5. Seetharam B, Tiruppathi C, Alpers DH. Hydrophobic interactions of brush border alkaline phosphatases: the role of phosphatidyl inositol. Arch Biochem Biophys. 1987;253:189–198.
6. Millán JL. *Mammalian Alkaline Phosphatases. From Biology to Applications in Medicine and Biotechnology*. Wiley-VCH, Weinheim, Germany: 2006.
7. Russell RG. Excretion of Inorganic Pyrophosphate in Hypophosphatasia. Lancet. 1965;2:461–464.
8. Russell RG, Bisaz S, Donath A, et al. Inorganic pyrophosphate in plasma in normal persons and in patients with hypophosphatasia, osteogenesis imperfecta, and other disorders of bone. J Clin Invest. 1971;50:961–969.
9. Whyte MP, Mahuren JD, Vrabel LA, et al. Markedly increased circulating pyridoxal-5′-phosphate levels in hypophosphatasia. Alkaline phosphatase acts in vitamin B6 metabolism. J Clin Invest. 1985;76: 752–756.
10. Whyte MP, Mahuren JD, Fedde KN, et al. Perinatal hypophosphatasia: tissue levels of vitamin B6 are unremarkable despite markedly increased circulating concentrations of pyridoxal-5′-phosphate. Evidence for an ectoenzyme role for tissue-nonspecific alkaline phosphatase. J Clin Invest. 1988;81:1234–1239.
11. McCance RA, Camb M, D, et al. The excretion of phosphoethanolamine and hypophosphatasia. Lancet. 1955;268:131.
12. Fleisch H, Maerki J, Russell RG. Effect of pyrophosphate on dissolution of hydroxyapatite and its possible importance in calcium homeostasis. Proc Soc Exp Biol Med. 1966;122:317–320.
13. Whyte MP, Valdes R Jr, Ryan LM, et al. Infantile hypophosphatasia: enzyme replacement therapy by intravenous infusion of alkaline phosphatase-rich plasma from patients with Paget bone disease. J Pediatr. 1982;101:379–386.
14. Whyte MP, McAlister WH, Patton LS, et al. Enzyme replacement therapy for infantile hypophosphatasia attempted by intravenous infusions of alkaline phosphatase-rich Paget plasma: results in three additional patients. J Pediatr. 1984;105:926–933.
15. Macpherson RI, Kroeker M, Houston CS. Hypophosphatasia. J Can Assoc Radiol. 1972;23:16–26.
16. Weninger M, Stinson RA, Plenk H Jr, et al. Biochemical and morphological effects of human hepatic alkaline phosphatase in a neonate with hypophosphatasia. Acta Paediatr Scand Suppl. 1989;360:154–160.
17. Whyte MP, Landt M, Ryan LM, et al. Alkaline phosphatase: placental and tissue-nonspecific isoenzymes hydrolyze phosphoethanolamine, inorganic pyrophosphate, and pyridoxal 5′-phosphate. Substrate accumulation in carriers of hypophosphatasia corrects during pregnancy. J Clin Invest. 1995;95:1440–1445.
18. Whyte MP, Kurtzberg J, McAlister WH, et al. Marrow cell transplantation for infantile hypophosphatasia. J Bone Miner Res. 2003;18:624–636.
19. Cahill RA, Wenkert D, Perlman SA, et al. Infantile hypophosphatasia: transplantation therapy trial using bone fragments and cultured osteoblasts. J Clin Endocrinol Metab. 2007;92:2923–2930.
20. Tadokoro M, Kanai R, Taketani T, et al. New bone formation by allogeneic mesenchymal stem cell transplantation in a patient with perinatal hypophosphatasia. J Pediatr. 2009;154:924–930.
21. Waymire KG, Mahuren JD, Jaje JM, et al. Mice lacking tissue nonspecific alkaline phosphatase die from seizures due to defective metabolism of vitamin B-6. Nat Genet. 1995;11:45–51.
22. Narisawa S, Frohlander N, Millán JL. Inactivation of two mouse alkaline phosphatase genes and establishment of a model of infantile hypophosphatasia. Dev Dyn. 1997;208:432–446.
23. Fedde KN, Blair L, Silverstein J, et al. Alkaline phosphatase knock-out mice recapitulate the metabolic and skeletal defects of infantile hypophosphatasia. J Bone Miner Res. 1999;14:2015–2026.
24. Hessle L, Johnson KA, Anderson HC, et al. Tissue-nonspecific alkaline phosphatase and plasma cell membrane glycoprotein-1 are central antagonistic regulators of bone mineralization. Proc Natl Acad Sci U S A. 2002;99:9445–9449.
25. Millán JL, Narisawa S, Lemire I, et al. Enzyme replacement therapy for murine hypophosphatasia. J Bone Miner Res. 2008;23:777–787.
26. Nishioka T, Tomatsu S, Gutierrez MA, et al. Enhancement of drug delivery to bone: characterization of human tissue-nonspecific alkaline phosphatase tagged with an acidic oligopeptide. Mol Genet Metab. 2006;88:244–255.
27. Ishizaki J, Waki Y, Takahashi-Nishioka T, et al. Selective drug delivery to bone using acidic oligopeptides. J Bone Miner Metab. 2009;27: 1–8.
28. Greenberg CR, Mhanni A, Catte D, et al. Interim results of adults and infants with hypophosphatasia treated with bone-targeted human recombinant alkaline phosphatase ENB-0040. Mol Genet Metab. 2009;98:7.
29. Sogabe N, Oda K, Nakamura H, et al. Molecular effects of the tissue-nonspecific alkaline phosphatase gene polymorphism (787T>C) associated with bone mineral density. Biomed Res. 2008;29:213–9.
30. Hanawa H, Yamamoto M, Zhao H, et al. Optimized lentiviral vector design improves titer and transgene expression of vectors containing

the chicken beta-globin locus HS4 insulator element. Mol Ther. 2009;17:667–674.

31. Segura MM, Kamen A, Garnier A. Downstream processing of oncoretroviral and lentiviral gene therapy vectors. Biotechnol Adv. 2006;24:321–337.
32. Kutner RH, Puthli S, Marino MP, et al. Simplified production and concentration of HIV-1-based lentiviral vectors using HYPERFlask vessels and anion exchange membrane chromatography. BMC Biotechnol. 2009;9:10.
33. Sastry L, Johnson T, Hobson MJ, Smucker B, Cornetta K. Titering lentiviral vectors: comparison of DNA, RNA and marker expression methods. Gene Ther. 2002;9:1155–1162.
34. Hanawa H, Hargrove PW, Kepes S, et al. Extended beta-globin locus control region elements promote consistent therapeutic expression of a gamma-globin lentiviral vector in murine beta-thalassemia. Blood. 2004;104:2281–2290.
35. Narisawa S, Wennberg C, Millán JL. Abnormal vitamin B6 metabolism in alkaline phosphatase knock-out mice causes multiple abnormalities, but not the impaired bone mineralization. J Pathol. 2001;193:125–133.
36. Goseki M, Oida S, Sasaki S. Detection of minor immunological differences among human "universal-type" alkaline phosphatases. J Cell Biochem. 1988;38:155–163.
37. Hoshi K, Amizuka N, Oda K, et al. Immunolocalization of tissue nonspecific alkaline phosphatase in mice. Histochem Cell Biol. 1997;107:183–191.
38. Sugiyama O, Orimo H, Suzuki S, et al. Bone formation following transplantation of genetically modified primary bone marrow stromal cells. J Orthop Res. 2003;21:630–637.
39. Murshed M, Harmey D, Millán JL, et al. Unique coexpression in osteoblasts of broadly expressed genes accounts for the spatial restriction of ECM mineralization to bone. Genes Dev. 2005;19:1093–1104.
40. Nienhuis AW, Dunbar CE, Sorrentino BP. Genotoxicity of retroviral integration in hematopoietic cells. Mol Ther. 2006;13:1031–1049.
41. Baumgartner-Sigl S, Haberlandt E, Mumm S, et al. Pyridoxine-responsive seizures as the first symptom of infantile hypophosphatasia caused by two novel missense mutations (c.677T>C, p.M226T; c.1112C>T, p.T371I) of the tissue-nonspecific alkaline phosphatase gene. Bone. 2007;40:1655–1661.

THE JOURNAL OF BIOLOGICAL CHEMISTRY VOL. 286, NO. 4, pp. 3094–3103, January 28, 2011

Cellular ATP Synthesis Mediated by Type III Sodium-dependent Phosphate Transporter *Pit-1* Is Critical to Chondrogenesis*

Received for publication, May 25, 2010, and in revised form, October 13, 2010 Published, JBC Papers in Press, November 12, 2010, DOI 10.1074/jbc.M110.148403

Atsushi Sugita[‡§], Shinji Kawai[¶], Tetsuyuki Hayashibara[‖], Atsuo Amano[¶], Takashi Ooshima[‖], Toshimi Michigami[**], Hideki Yoshikawa[§], and Toshiyuki Yoneda[‡1]

From the Departments of [‡]Biochemistry, [¶]Oral Frontier Biology, and [‖]Pediatric Dentistry, Osaka University Graduate School of Dentistry, and the [**]Department of Bone and Mineral Research, Osaka Medical Center and Research Institute for Maternal and Child Health, Izumi, Osaka 594-1101, Japan and the [§]Department of Orthopaedic Surgery, Osaka University Graduate School of Medicine, Suita, Osaka 565-0871, Japan

Disturbed endochondral ossification in X-linked hypophosphatemia indicates an involvement of P_i in chondrogenesis. We studied the role of the sodium-dependent P_i cotransporters (NPT), which are a widely recognized regulator of cellular P_i homeostasis, and the downstream events in chondrogenesis using *Hyp* mice, the murine homolog of human X-linked hypophosphatemia. *Hyp* mice showed reduced apoptosis and mineralization in hypertrophic cartilage. *Hyp* chondrocytes in culture displayed decreased apoptosis and mineralization compared with WT chondrocytes, whereas glycosaminoglycan synthesis, an early event in chondrogenesis, was not altered. Expression of the type III NPT *Pit-1* and P_i uptake were diminished, and intracellular ATP levels were also reduced in parallel with decreased caspase-9 and caspase-3 activity in *Hyp* chondrocytes. The competitive NPT inhibitor phosphonoformic acid and ATP synthesis inhibitor 3-bromopyruvate disturbed endochondral ossification with reduced apoptosis *in vivo* and suppressed apoptosis and mineralization in conjunction with reduced P_i uptake and ATP synthesis in WT chondrocytes. Overexpression of *Pit-1* in *Hyp* chondrocytes reversed P_i uptake and ATP synthesis and restored apoptosis and mineralization. Our results suggest that cellular ATP synthesis consequent to P_i uptake via *Pit-1* plays an important role in chondrocyte apoptosis and mineralization, and that chondrogenesis is ATP-dependent.

Endochondral ossification is critical to the development and growth of mammals. The process begins with condensation of undifferentiated mesenchymal cells, and these cells differentiate into proliferating chondrocytes that express type II, IX, and XI collagen and sulfated glycosaminoglycans (GAG)[2] (1). Proliferating chondrocytes further differentiate into hypertrophic chondrocytes expressing type X collagen, undergo apoptosis, mineralize, and are ultimately replaced by bone. Disturbance of the endochondral ossification leads to a variety of skeletal disorders.

The genetic disease X-linked hypophosphatemia (XLH) is the most common form of inherited rickets in humans and is related to the dominant disorder of P_i homeostasis (2). XLH has been shown to be caused by inactive mutations of the *PHEX* gene and characterized by hypophosphatemia secondary to renal P_i wasting, growth retardation due to disturbed endochondral ossification, osteomalacia resulting from reduced mineralization, and abnormally regulated vitamin D metabolism (3). *Hyp* mice also display similar biochemical and phenotypic abnormalities to human XLH, including hypophosphatemia, osteomalacia, and skeletal abnormalities. *Hyp* mice thus are a mouse homolog of human XLH (4). Previous studies reported that *Hyp* mice exhibited disorganized hypertrophic cartilage with reduced apoptotic chondrocytes and hypomineralization (5). We have reported previously that osteoclast number was decreased in *Hyp* mice compared with WT mice and that a high-P_i diet partially restored this, showing that P_i influences osteoclastogenesis and suggesting that this P_i effect on osteoclastogenesis may be associated with the pathogenesis of abnormal skeletogenesis in *Hyp* mice (6). However, it remains unclear whether disturbed P_i homeostasis influences endochondral ossification, leading to abnormal skeletogenesis in *Hyp* mice. In this context, it is noted that intracellular P_i levels decrease and extracellular P_i levels prominently increase from the proliferating to the hypertrophic zone during chondrogenesis, suggesting that cellular P_i levels are associated with chondrocyte differentiation (7–10).

Cellular P_i levels are controlled by the sodium-dependent P_i cotransporters (NPT) (11). Previous studies reported that the type III NPT *Pit-1* was expressed in hypertrophic chondrocytes during endochondral ossification in mice (12) and that the expression of the type IIa NPT *Npt2a* and *Pit-1* was also detected in chick chondrocytes (13). Moreover, it has been demonstrated that P_i modulates chondrocyte differentiation (14–19) and apoptosis (13, 20).

On the basis of these earlier results, we hypothesized that the NPT-P_i system plays a critical role in the regulation of chondrocyte differentiation. We found that *Pit-1* expression in chondrocytes was decreased in *Hyp* mice compared with WT mice and that *Pit-1* regulated apoptosis and mineralization in chondrocytes through modulating intracellular ATP

* This work was supported in part by the 21st Century COE Program entitled "Origination of Frontier BioDentistry" at Osaka University Graduate School of Dentistry, by the Ministry of Education, Culture, Sports, Science, and Technology, and by Grant-in-aid for Scientific Research A202290100 from the Japanese Society for the Promotion of Science (to T. Y.).

[1] To whom correspondence should be addressed: 1-8 Yamadaoka, Suita, Osaka 565-0871, Japan. Fax: 81-6-6879-2890; E-mail: tyoneda@dent.osaka-u.ac.jp.

[2] The abbreviations used are: GAG, glycosaminoglycan(s); XLH, X-linked hypophosphatemia; NPT, sodium-dependent P_i cotransporter(s); PFA, phosphonoformic acid; 3-BrPA, 3-bromopyruvate; STC, stanniocalcin.

synthesis and apoptotic signaling activity. On the other hand, *Hyp* chondrocytes showed no changes in GAG synthesis, which is an early event in chondrogenesis. Our findings suggest that ATP synthesis mediated by P_i influx via *Pit-1* is critical in the regulation of late chondrogenesis, including apoptosis and mineralization, and that the differentiation of cartilage is an ATP-dependent event.

EXPERIMENTAL PROCEDURES

Animals—All mice used were of the C57BL/6J strain. Normal mice were purchased from Nihon-Dobutsu Inc. (Osaka, Japan). *Hyp* mice were initially obtained from The Jackson Laboratory (Bar Harbor, ME) and were produced by crossmating homozygous *Hyp* females (*Hyp*/*Hyp*) with hemizygous *Hyp* males (*Hyp*/Y). All animal experiments were performed according to the guidelines of the Institutional Animal Care and Use Committee of the Osaka University Graduate School of Dentistry.

Isolation and Culture of Mouse Growth Plate Chondrocytes—Growth plate chondrocytes were isolated from the ribs of 4-week-old normal and *Hyp* mice by sequential digestion with 0.2% trypsin (Invitrogen) for 30 min and 0.2% collagenase (Wako Pure Chemical Industries Ltd., Osaka, Japan) for 3 h as reported previously (21). Isolated cells were plated onto 100-mm tissue culture dishes at a density of 1×10^6 cells in α-minimal essential medium (Sigma) supplemented with 10% FCS (Valley Biomedical, Inc., Winchester, VA), 2 mmol/liter L-glutamine, and 0.1 mg/ml kanamycin. Two days later, to induce chondrogenesis and cartilage nodule formation, the cells were plated at 3×10^5 cells/well onto 24-well plates or at 5×10^4 cells/well on 96-well plates coated with type I collagen (Nitta Gelatin Inc., Osaka, Japan) and cultured in differentiation medium consisting of DMEM (Sigma) supplemented with 10% FCS, 50 μg/ml ascorbic acid, and 100 ng/ml recombinant human bone morphogenetic protein-2 (Astellas Pharma Inc., Tokyo, Japan) for 7 days. From day 5 to day 7, to promote matrix mineralization, 5 mM β-glycerophosphate was added to the differentiation medium.

RT-PCR and Real-time PCR—Total RNA from chondrocytes was prepared using an RNeasy kit (Qiagen, Inc., Valencia, CA) and reverse-transcribed with SuperScript II reverse transcriptase (Invitrogen). The primer sequences for mouse *Npt1*, mouse *Npt2a*, GAPDH, and β-actin are available on request. PCR assays were performed using *Taq* DNA polymerase (New England Biolabs, Ipswich, MA) and dNTP mixture (Promega Corp., Madison, WI). Real-time PCR assays were performed using a LightCycler system (Roche Diagnostics) according to the manufacturer's instructions. Each reaction was carried out with Qiagen QuantiTect SYBR Green PCR Master Mix. The expression levels of mRNA are indicated as the relative expression normalized by GAPDH. The primer sequences are available upon request. Each procedure was repeated at least four times to assess reproducibility.

Measurement of Sodium-dependent P_i Uptake—Assay for sodium-dependent P_i uptake by growth plate chondrocytes was performed essentially as described (22). Briefly, confluent cells cultured in 24-well Costar microtiter dishes were incubated in 2 ml of uptake solution (150 mmol/liter NaCl, 1.0 mmol/liter $CaCl_2$, 1.8 mmol/liter $MgSO_4$, and 10 mmol/liter HEPES (pH 7.4)) at 37 °C for 5 min. Transport was then initiated by replacing the uptake solution with fresh uptake solution (2 ml) supplemented with 0.1 mmol/liter KH_2PO_4 and containing 3 μCi/ml $KH_2{}^{32}PO_4$ (MP Biomedicals, Inc., Irvine, CA). Cells were then incubated for 5 min at 37 °C, and the reaction was stopped by the addition of ice-cold uptake solution supplemented with 150 mmol/liter choline chloride substitution for NaCl. The same solution was then used to wash the cells three times (2 ml/wash) and dissolved in 0.2 N NaOH, and the ^{32}P activity was counted on a scintillation counter. As a control, sodium-independent P_i transport was measured in the same way, except that NaCl was replaced by choline chloride in the uptake solution. Data are expressed as nanomoles of P_i/mg of cellular protein/5 min, and sodium-dependent P_i transport was calculated by subtracting sodium-independent P_i transport from total P_i transport.

Alcian Blue Staining—Cell layers in 24-well plates were fixed with 3.7% formaldehyde for 10 min and with 70% ethanol for 5 min at room temperature. After fixation, the cells were incubated with 5% acetic acid (pH 1.0, adjusted with HCl) for 5 min and stained with 1% Alcian blue dye (Wako Pure Chemical Industries Ltd.) in 5% acetic acid for 10 min. The Alcian blue staining was quantified using NIH Image 1.63 software.

Alizarin Red Staining—Cell layers in 24-well plates were fixed with 3.7% formaldehyde for 10 min and with 95% ethanol for 10 min at room temperature. After fixation, mineralized nodules were stained with 1% alizarin red S (Wako Pure Chemical Industries Ltd.) at pH 6.4 for 10 min at room temperature. The stained samples were washed three times with water and then air-dried. The alizarin red staining was quantified using NIH Image 1.63 software.

Treatment with NPT Inhibitor—*In vitro*, chondrocytes were treated with phosphonoformic acid (PFA or foscarnet, Sigma), which is a competitive inhibitor of NPT (23), at concentrations of 10^{-5} to 10^{-3} M in the differentiation medium from day 1 to day 7. *In vivo*, mice received PFA as described (24). PFA injection (intraperitoneal; 1000 mg/kg of body weight) was started at 21 days of age and injected daily for 10 days into C57BL/6J mice. Histological analysis was performed at 31 days of age. Control mice received vehicle PBS.

Knockdown of Npt2a and Pit-1 by siRNA—Chondrocytes were seeded at a density of 5×10^5 cells in 100-mm tissue culture dishes in α-minimal essential medium supplemented with 10% FCS and 2 mmol/liter L-glutamine. The sequences of Stealth RNAi duplex oligoribonucleotides for mouse *Npt2a* and mouse *Pit-1* are available upon request. *Npt2a*-targeted, *Pit-1*-targeted, or negative control (medium GC, Invitrogen) Stealth RNAi duplex oligoribonucleotides were each added to 1 ml of serum-free Opti-MEM I reduced serum medium (Invitrogen) at a final concentration of 24 nM. In a separate tube, 20 μl of Lipofectamine RNAiMAX (Invitrogen) were diluted in 1 ml of serum-free Opti-MEM I reduced serum medium. After adding the siRNA solution to the Lipofectamine solution, the final transfection mixture was incubated for 20 min at room temperature. This transfection mixture was applied to the cells. After 48 h, RNA extraction was performed for

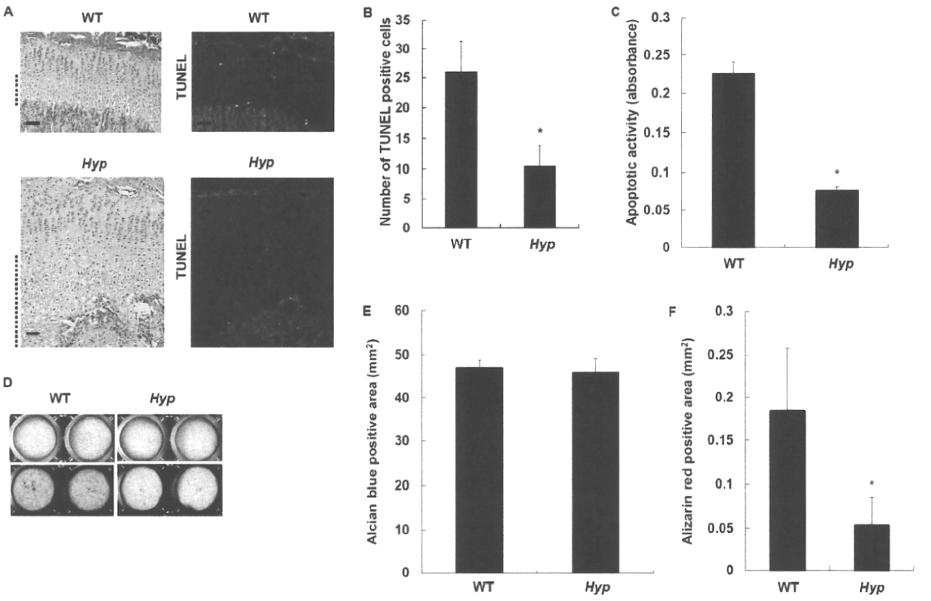

FIGURE 1. **Apoptosis and related events in *Hyp* chondrocytes.** *A*, histological examination of chondrocyte apoptosis. Hematoxylin/eosin staining (*left*) and TUNEL staining (*right*) were performed using tibias of 4-week-old WT and *Hyp* mice. The hypertrophic zone is marked with *dotted lines*, and the *scale bars* indicate 200 μm. Representative pictures obtained of numerous sections of four mice from each group are shown. *B*, number of TUNEL-positive cells in the tibial growth plates of WT and *Hyp* mice. *C*, quantitative determination of chondrocyte apoptosis. Cells were cultured in the differentiation medium in 96-well plates for 7 days. The determination was conducted using the cell death detection ELISA^{PLUS} kit after differentiation. Data are shown as apoptotic activity. *D*, histochemical staining of WT and *Hyp* chondrocytes. Cells were cultured for 7 days in the differentiation medium and stained with Alcian blue for GAG synthesis (*upper*) and with alizarin red S for mineralization (*lower*). *E*, quantification of Alcian blue staining. *F*, quantification of alizarin red staining. Results are expressed as the mean ± S.E. of four separate experiments. *, significantly different from WT chondrocytes ($p < 0.05$).

RT-PCR, and transfected chondrocytes were plated onto 24- or 96-well plates to determine P_i transport, intracellular ATP levels, caspase activity, and apoptosis.

Pit-1 Overexpression—The cDNA was subcloned into the 5′-XhoI/BamHI-3′ site of pcDNA3.1/Zeo (Invitrogen). The cells were transfected using FuGENE^{TM}-6 (Roche Diagnostics) according to the manufacturer's protocol. After 48 h of transfection, RNA extraction was performed for RT-PCR, or transfected chondrocytes were replated onto 24- or 96-well plates to determine P_i transport, intracellular ATP levels, caspase activity, and apoptosis. The cDNA for mouse *Pit-1* in the plasmid pBluescript was a generous gift of Dr. Kenichi Miyamoto (University of Tokushima Graduate School, Tokushima, Japan).

Histology and TUNEL Staining—Tibias were harvested, washed with PBS, fixed with 4% paraformaldehyde in 0.1 M phosphate buffer (pH 7.4) overnight, decalcified in 4.13% EDTA at room temperature for 2 weeks, and embedded in paraffin. Four-μm thick sections were made and stained with hematoxylin and eosin. Apoptotic cells were identified using the DeadEnd fluorometric TUNEL system (Promega Corp.). After treatment with 10 mg/ml proteinase K for 10 min at room temperature, sections were incubated with rTdT incubation buffer for 1 h at 37 °C, rinsed, counterstained with 1 μg/ml DAPI (Vector Laboratories, Ltd., Burlingame, CA), and mounted with Fluoromount-G (Southern Biotechnology Associates, Inc., Birmingham, AL). The green TUNEL emission was analyzed under a fluorescein filter set to view the green fluorescence of fluorescein at 520 nm and blue DAPI at 460 nm.

Measurement of Apoptotic Cell Death—DNA fragmentation was measured using the cell death detection ELISA^{PLUS} kit (Roche Diagnostics), which detects the cytoplasmic histone-associated DNA fragments (mono- and oligonucleosomes) by photometric enzyme immunoassay. Briefly, after differentiation of chondrocytes in 96-well plates, cell lysates were used for the ELISA procedure following the manufacturer's protocol. DNA fragmentation was quantified at 405 nm. Results were normalized to cellular protein concentration.

Measurement of Caspase-9 and Caspase-3 Activity—Activity of caspase-3 and caspase-9 was measured using the Caspase-Glo 3/7 and Caspase-Glo 9 assay kit (Promega corp.) according to the manufacturer's instructions. Chondrocytes were cultured at a density of 5×10^4 cells/well for 5 days in 96-well plates in the differentiation medium and processed for caspase-9 and caspase-3 activity assays. The luminescence was measured using a TD-20/20 luminometer (Tuner Designs, Sunnyvale, CA). Results were normalized to cellular protein concentration.

Measurement of Intracellular ATP Levels—Intracellular ATP levels were measured using an ATP assay kit (Calbiochem). This assay utilizes luciferase to catalyze the formation of light from ATP and luciferin. Luminescence was measured using a TD-20/20 luminometer. Chondrocytes were cultured at a density of 5×10^4 cells/well for 24 h in 24-well plates and processed for ATP bioluminescence assays. Results were normalized to cellular protein concentration.

Treatment with ATP Synthesis Inhibitor—*In vitro*, 3-bromopyruvate (3-BrPA; Sigma), a strong alkylating agent that abolishes cell ATP production via the inhibition of both gly-

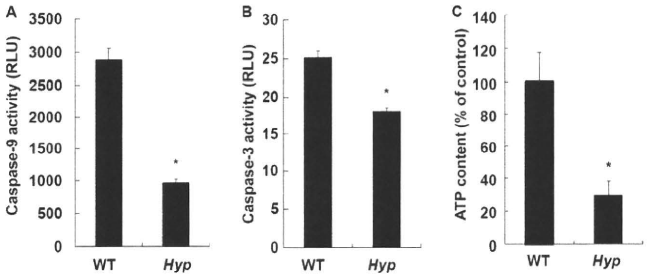

FIGURE 2. **Activity of apoptotic signaling pathways.** *A*, caspase-9 activity in WT and *Hyp* chondrocytes. *B*, caspase-3 activity in WT and *Hyp* chondrocytes. Activity was measured using the Caspase-Glo 9 and Caspase-Glo 3/7 assay kits after differentiation. *C*, intracellular ATP levels in WT and *Hyp* chondrocytes. Cells were cultured at a density of 1×10^4 cells/well in 96-well plates for 24 h. ATP levels were measured using the ATP assay kit. *, significantly different from WT chondrocytes ($p < 0.05$). *RLU*, relative light units.

colysis and oxidative phosphorylation (25–27), was added at 10^{-6}~10^{-5} M in the differentiation medium from day 1 to day 7. *In vivo*, 3-BrPA (20 μg/kg of body weight) was injected intraperitoneally daily for 10 days into C57BL/6J mice. Control mice received vehicle PBS.

Statistical Analysis—Data are presented as the mean ± S.E. Raw data were analyzed by the Mann-Whitney *U* test or one-way analysis of variance, followed by a post hoc test (Fisher's projected least significant difference) (StatView, SAS Institute, Inc., Cary, NC) with a significance level of $p < 0.05$.

RESULTS

Reduced Apoptosis and Mineralization in Growth Plate Cartilage in Hyp Mice—It has been reported that apoptosis is a prerequisite to mineralization of chondrocytes (28). Previous studies, including ours, have reported that the growth plate cartilage in *Hyp* mice is hypomineralized (5, 6). We therefore examined apoptosis in the growth plate cartilage in *Hyp* mice compared with WT mice. Histological examination revealed that hypertrophic cartilage was elongated and disorganized in *Hyp* mice (Fig. 1*A*, *left*). In conjunction with this, TUNEL staining showed decreased apoptosis in hypertrophic cartilage in *Hyp* mice (Fig. 1, *A* (*right*) and *B*). Consistent with these *in vivo* results, chondrocytes isolated from *Hyp* mice (*Hyp* chondrocytes) in culture showed decreased apoptosis assessed by DNA fragmentation using a commercially available ELISA kit (Fig. 1*C*), and mineralization was determined by alizarin red staining (Fig. 1*D*, *lower*). Quantification of alizarin red staining is shown in Fig. 1*F*. However, GAG synthesis, which takes place at an early stage of chondrogenesis, was not altered in *Hyp* chondrocytes as determined by Alcian blue staining (Fig. 1*D*, *upper*) Alcian blue staining is quantified in Fig. 1*E*.

Cellular Events Involved in Reduced Apoptosis in Hyp Chondrocytes—Because activation of caspase-9 and caspase-3 is an important step that leads to apoptosis, the activity of caspase-9 and caspase-3 was next determined in WT and *Hyp* chondrocytes in culture. The activity of caspase-9 (Fig. 2*A*) and caspase-3 (Fig. 2*B*) was significantly decreased in *Hyp* chondrocytes. ATP has been reported to be critical in the activation of caspase-9 and caspase-3 (29, 30). Accordingly, we determined intracellular ATP levels in WT and *Hyp* chondrocytes and found that intracellular ATP levels in *Hyp* chondrocytes were significantly reduced compared with WT chondrocytes (Fig. 2*C*). Collectively, these results suggest that decreased ATP levels impaired caspase signals following apoptosis in *Hyp* chondrocytes.

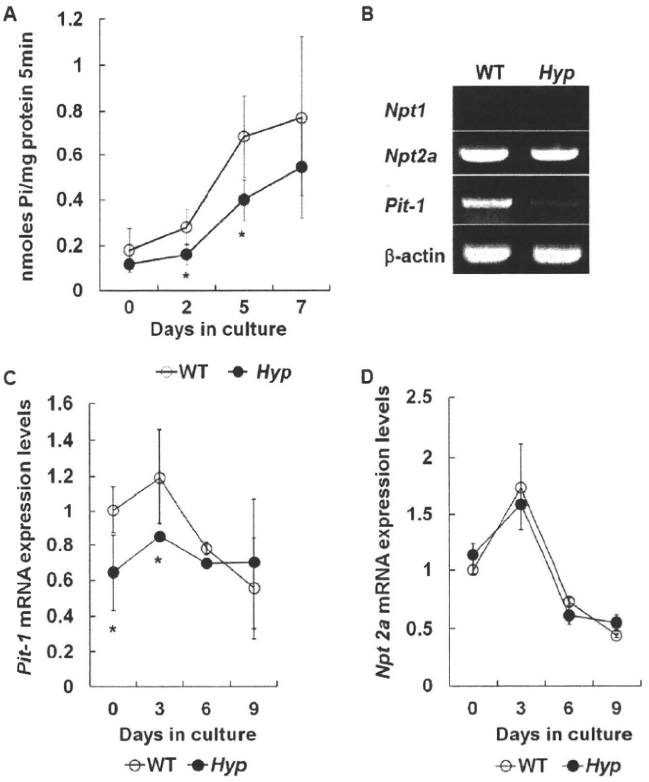

FIGURE 3. **Characterization of *Hyp* chondrocytes.** *A*, time course of P_i uptake in WT (○) and *Hyp* (●) chondrocytes. The cells were cultured for 7 days in the differentiation medium, and P_i uptake was determined as described under "Experimental Procedures." *B*, expression of *Npt1*, *Npt2a*, and *Pit-1* mRNAs in WT and *Hyp* chondrocytes. Total RNA isolated from chondrocytes cultured for 24 h was used for RT-PCR analysis using the primer pairs. β-Actin was amplified as a control. *C*, time-dependent expression of *Pit-1* mRNA by real-time PCR. *D*, time-dependent expression of *Npt2a* mRNA by real-time PCR. The amount of *Npt2a* and *Pit-1* of WT chondrocytes at day 0 was designated as 1.0 and normalized to GAPDH. Results are expressed as the mean ± S.E. of four separate experiments. *, significantly different from WT chondrocytes ($p < 0.05$).

Disturbed P_i Homeostasis in Hyp Chondrocytes—It has been described that P_i is a source of ATP (31). Accordingly, we next examined whether P_i uptake was changed in *Hyp* chondrocytes. As expected, we found that P_i uptake was significantly less in *Hyp* chondrocytes than in WT chondrocytes (Fig. 3*A*). Because cellular P_i uptake is under the control of NPT (11), NPT expression in *Hyp* chondrocytes was subsequently determined. RT-PCR showed that the type III NPT *Pit-1* expression was decreased in *Hyp* chondrocytes (Fig. 3*B*), and real-time PCR demonstrated that *Pit-1* expression was reduced at the early stages of chondrocyte culture (Fig. 3*C*). Consistent with our results, previous studies also reported that an increase in *Pit-1* expression at an early stage was associated with late chondrocyte differentiation (16, 18). On the other hand, there was no difference in the type II *Npt2a* expression between WT and *Hyp* chondrocytes (Fig. 3, *B* and *D*). The type I *Npt1* expression was not detected in WT and *Hyp* chondrocytes (Fig. 3*B*). These results suggest that P_i up-

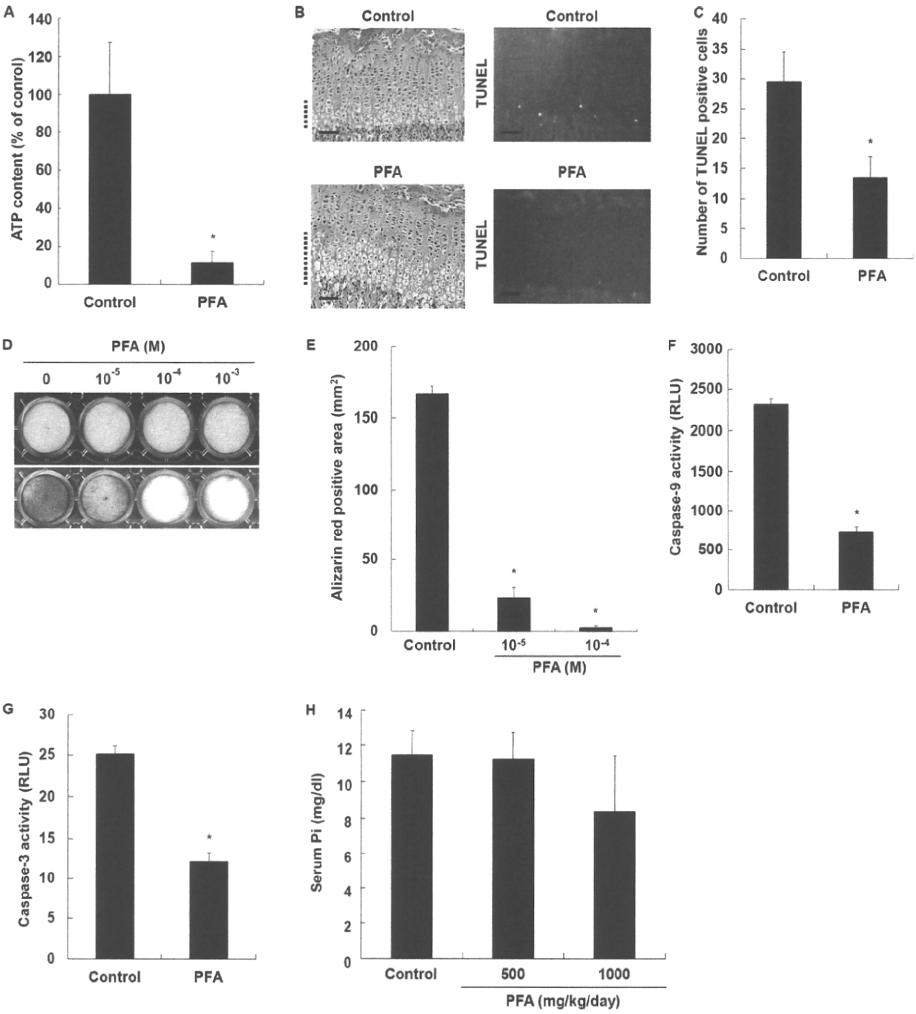

FIGURE 4. **Effects of PFA on chondrocyte differentiation.** *A*, intracellular ATP levels. Cells were cultured in the presence of 10^{-5} M PFA. ATP levels were measured using the ATP assay kit. *B*, histological examination of chondrocyte apoptosis. Hematoxylin/eosin staining (*left*) and TUNEL staining (*right*) were performed on tibial sections from 31-day-old control and PFA-treated mice. The hypertrophic zone is marked with *dotted lines*, and the *scale bars* indicate 200 μm. Representative pictures obtained of numerous sections of four mice from each group are shown. *C*, number of TUNEL-positive cells in the tibial growth plates of control and PFA-treated mice. *D*, histochemical staining of chondrocytes. Cells were cultured in the presence of 10^{-5} M PFA and stained with Alcian blue for GAG synthesis (*upper*) and alizarin red S for mineralization (*lower*). *E*, quantification of alizarin red staining. *F*, caspase-9 activity. *G*, caspase-3 activity. Cells were cultured in the presence of 10^{-5} M PFA. Activity was measured using the Caspase-Glo 9 and Caspase-Glo 3/7 assays. *H*, serum P_i levels. Results are expressed as the mean ± S.E. of four separate determinations. *, significantly different from control ($p < 0.05$). *RLU*, relative light units.

take via *Pit-1* is specifically involved in the regulation of chondrogenesis, including apoptosis and mineralization.

Suppression of Chondrocyte Differentiation by NPT Inhibitor—To verify whether a decrease in P_i uptake due to reduced *Pit-1* expression is responsible for a reduction in ATP levels in *Hyp* chondrocytes, we determined the effects of PFA (foscarnet), which is a competitive inhibitor of P_i uptake via NPT (23), on intracellular ATP levels. PFA (10^{-5} to 10^{-3} M) reduced P_i uptake in chondrocytes in a dose-dependent manner (data not shown). PFA (10^{-5} M) profoundly reduced intracellular ATP levels (Fig. 4*A*). Of note, PFA treatment caused disorganization of growth plate cartilage (Fig. 4*B*, *left*) and significantly decreased the number of TUNEL-positive chondrocytes in hypertrophic cartilage (Fig. 4, *B* (*right*) and *C*) in a similar manner to that seen in *Hyp* mice. Consistent with these *in vivo* results, PFA markedly inhibited mineralization of chondrocytes in a dose-dependent manner (Fig. 4, *D* (*lower*) and *E*), whereas GAG synthesis was not affected by PFA treatment (Fig. 4*D*, *upper*). Furthermore, PFA also inhibited caspase-9 (Fig. 4*F*) and caspase-3 (Fig. 4*G*) activity. We determined serum P_i levels in PFA-treated mice. There was a trend of decreased serum P_i levels in PFA-treated mice, but it was not significantly different (Fig. 4*H*). The results are consistent with the notion that P_i uptake via *Pit-1* is closely associated with late chondrogenesis, including apoptosis and mineralization, through reducing ATP synthesis. These results also suggest an important role for intracellular P_i over extracellular P_i in the regulation of apoptosis and ATP synthesis in chondrocytes.

Suppression of Chondrocyte Differentiation by NPT siRNA—To further and more specifically verify the role of *Pit-1* in chondrocyte differentiation, we performed knockdown experiments using siRNA for *Pit-1*. As control, *Npt2a* was also knocked down. *Pit-1* and *Npt2a* siRNAs profoundly reduced

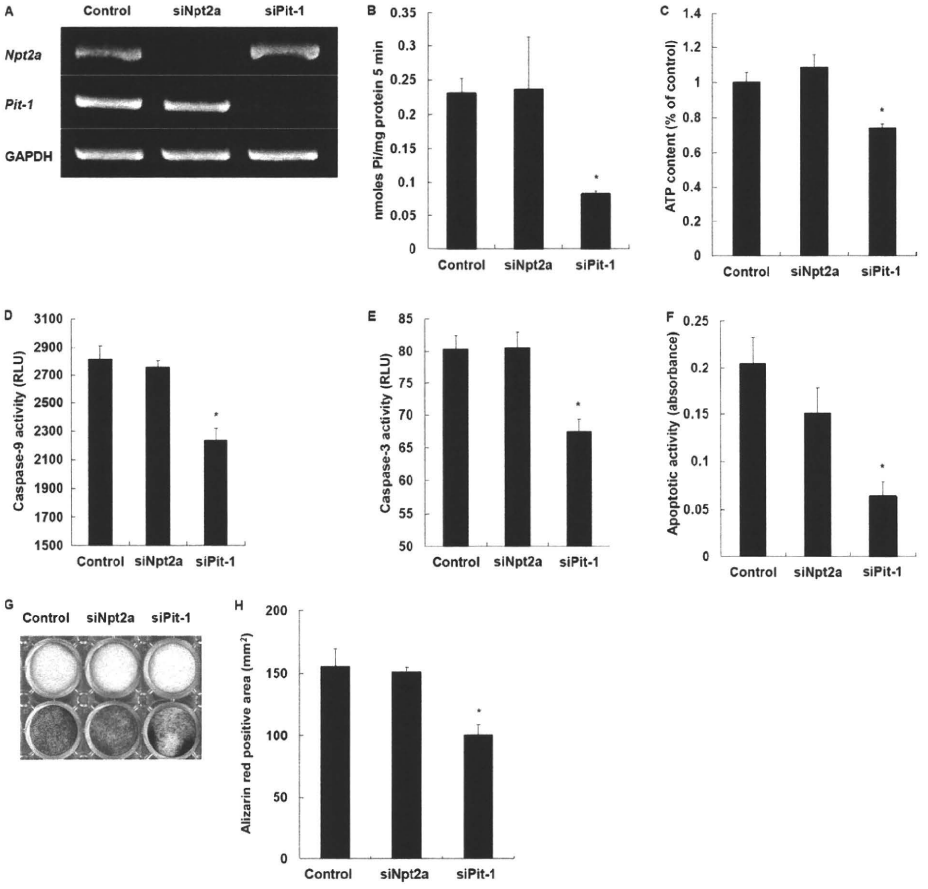

FIGURE 5. ***Npt2a* and *Pit-1* knockdown by siRNA in chondrocytes.** *A*, negative control, *Npt2a*, or *Pit-1* siRNA was transfected in chondrocytes, and the expression of *NPT2a*, *Pit-1*, or GAPDH was analyzed by RT-PCR. *B*, P_i uptake in negative control, *Npt2a* (*siNpt2a*), and *Pit-1* (*siPit-1*) siRNA-transfected chondrocytes was determined in the presence of 3 μCi/ml $KH_2{}^{32}PO_4$. *C*, intracellular ATP levels in negative control, *Npt2a*, and *Pit-1* siRNA-transfected chondrocytes. *D*, caspase-9 activity in negative control, *Npt2a*, and *Pit-1* siRNA-transfected chondrocytes. *E*, caspase-3 activity in negative control, *Npt2a*, and *Pit-1* siRNA-transfected chondrocytes. *F*, quantitative determination of chondrocyte apoptosis in negative control, *Npt2a*, and *Pit-1* siRNA-transfected chondrocytes. *G*, histochemical staining of negative control, *Npt2a*, and *Pit-1* siRNA-transfected chondrocytes. Cells were cultured and stained with Alcian blue for GAG synthesis (*upper*) and alizarin red S for mineralization (*lower*). *H*, quantification of alizarin red staining. We repeated the experiments twice using different preparations of primary chondrocytes and obtained identical results. Results are expressed as the mean ± S.E. of two separate determinations. *, significantly different from control ($p < 0.05$). *RLU*, relative light units.

Pit-1 and *Npt2a* mRNA levels in WT chondrocytes, respectively (Fig. 5*A*). *Pit-1* knockdown by *Pit-1* siRNA significantly decreased P_i uptake (Fig. 5*B*), intracellular ATP levels (Fig. 5*C*), and caspase-9 (Fig. 5*D*) and caspase-3 (Fig. 5*E*) activity. In parallel with these, apoptosis (Fig. 5*F*) and mineralization (Fig. 5, *G* and *H*) were also suppressed. In contrast, knockdown of *Npt2a* by *Npt2a* siRNA had no effects on apoptosis, mineralization, and other determinations (Fig. 5, *B–H*). These data suggest that *Pit-1* specifically controls P_i uptake following cascades of ATP-dependent caspase signaling, apoptosis, and mineralization in chondrocytes.

Recovery of Differentiation in Hyp Chondrocytes by Pit-1 Overexpression—As an alternative approach to confirm a critical role of *Pit-1* in apoptosis and mineralization in chondrocytes, we next examined the effects of *Pit-1* overexpression on *Hyp* chondrocytes. *Pit-1* overexpression significantly increased P_i uptake (Fig. 6*A*) and intracellular ATP levels (Fig. 6*B*) in *Hyp* chondrocytes. Furthermore, *Pit-1* overexpression also stimulated caspase-9 (Fig. 6*C*) and caspase-3 (Fig. 6*D*) activity, apoptosis (Fig. 6*E*), and mineralization (Fig. 6, *F* and *G*). WT chondrocytes also showed significantly increased P_i uptake (Fig. 6*A*), intracellular ATP levels (Fig. 6*B*), caspase-9 (Fig. 6*C*) and caspase-3 (Fig. 6*D*) activity, apoptosis (Fig. 6*E*), and mineralization (Fig. 6, *F* and *G*) by *Pit-1* overexpression. These results further suggest that *Pit-1* is critical in the regulation of P_i uptake and following cascades of ATP-dependent caspase signaling, apoptosis, and mineralization in chondrocytes.

Suppression of Chondrocyte Differentiation by ATP Synthesis Inhibitor—To further examine the role of intracellular ATP in chondrocyte differentiation, we studied the effects of the ATP synthesis inhibitor 3-BrPA. 3-BrPA (10^{-6} M) significantly reduced intracellular ATP levels in WT chondrocytes in culture (data not shown). Caspase-9 (Fig. 7*A*) and caspase-3 (Fig. 7*B*) activity was also significantly decreased in 3-BrPA-treated chondrocytes. More importantly, 3-BrPA treatment significantly decreased the number of TUNEL-positive chondrocytes in the hypertrophic zone in mice (Fig. 7, *C* and *D*). 3-BrPA inhibited chondrocyte mineralization in a dose-dependent manner (Fig. 7, *E* and *F*). However, GAG synthesis was not affected by 3-BrPA (Fig. 7*E*). The serum P_i levels in 3-BrPA-treated mice were not significantly different from those in control mice (Fig. 7*G*), suggesting an important role

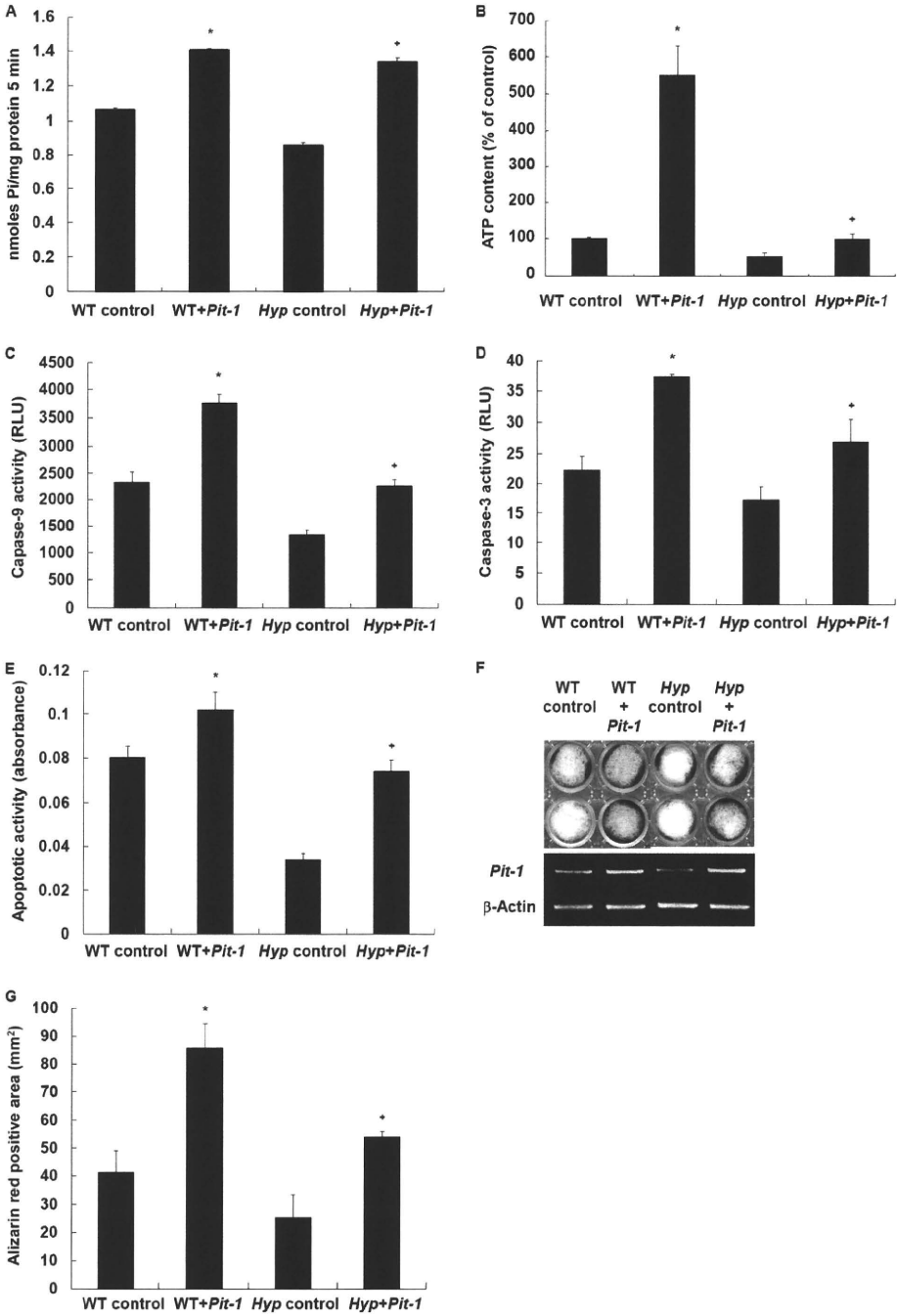

FIGURE 6. **Effects of *Pit-1* overexpression in chondrocytes.** *A*, empty vector (control) or *Pit-1* was transfected in WT and *Hyp* chondrocytes. P_i uptake was determined in the presence of 3 μCi/ml $KH_2{}^{32}PO_4$. *B*, intracellular ATP levels in control or *Pit-1*-transfected WT and *Hyp* chondrocytes. *C*, caspase-9 activity in control and *Pit-1*-transfected WT and *Hyp* chondrocytes. *D*, caspase-3 activity in control and *Pit-1*-transfected WT and *Hyp* chondrocytes. *E*, quantitative determination of apoptosis in control and *Pit-1*-transfected WT and *Hyp* chondrocytes. *F*, histochemical staining of control and *Pit-1*-transfected WT and *Hyp* chondrocytes. Cells were cultured and stained with alizarin red S for mineralization. *Pit-1* expression was confirmed by RT-PCR. *G*, quantification of alizarin red staining. We repeated the experiments twice using different preparations of primary chondrocytes and obtained identical results. Results are expressed as the mean ± S.E. of two separate determinations. *, significantly different from WT control ($p < 0.05$). +, significantly different from *Hyp* control ($p < 0.05$). *RLU*, relative light units.

for intracellular P_i over extracellular P_i. These results suggest that ATP synthesis is important for chondrocytes to undergo apoptosis via caspase signaling and advance to mineralization.

DISCUSSION

In this study, we explored the role of the P_i-NPT system in chondrogenesis using *Hyp* mice compared with WT mice. We found that *Hyp* mice exhibited a widened and disorganized hypertrophic zone with reduced chondrocyte apoptosis compared with WT mice. In addition, PFA (a competitive inhibitor of *Pit-1*) or 3-BrPA (an ATP synthesis inhibitor) markedly caused elongation and disorganization of hypertrophic cartilage with reduced apoptosis in WT mice in a similar manner to that in *Hyp* mice. It is noted that the disorders in the hy-

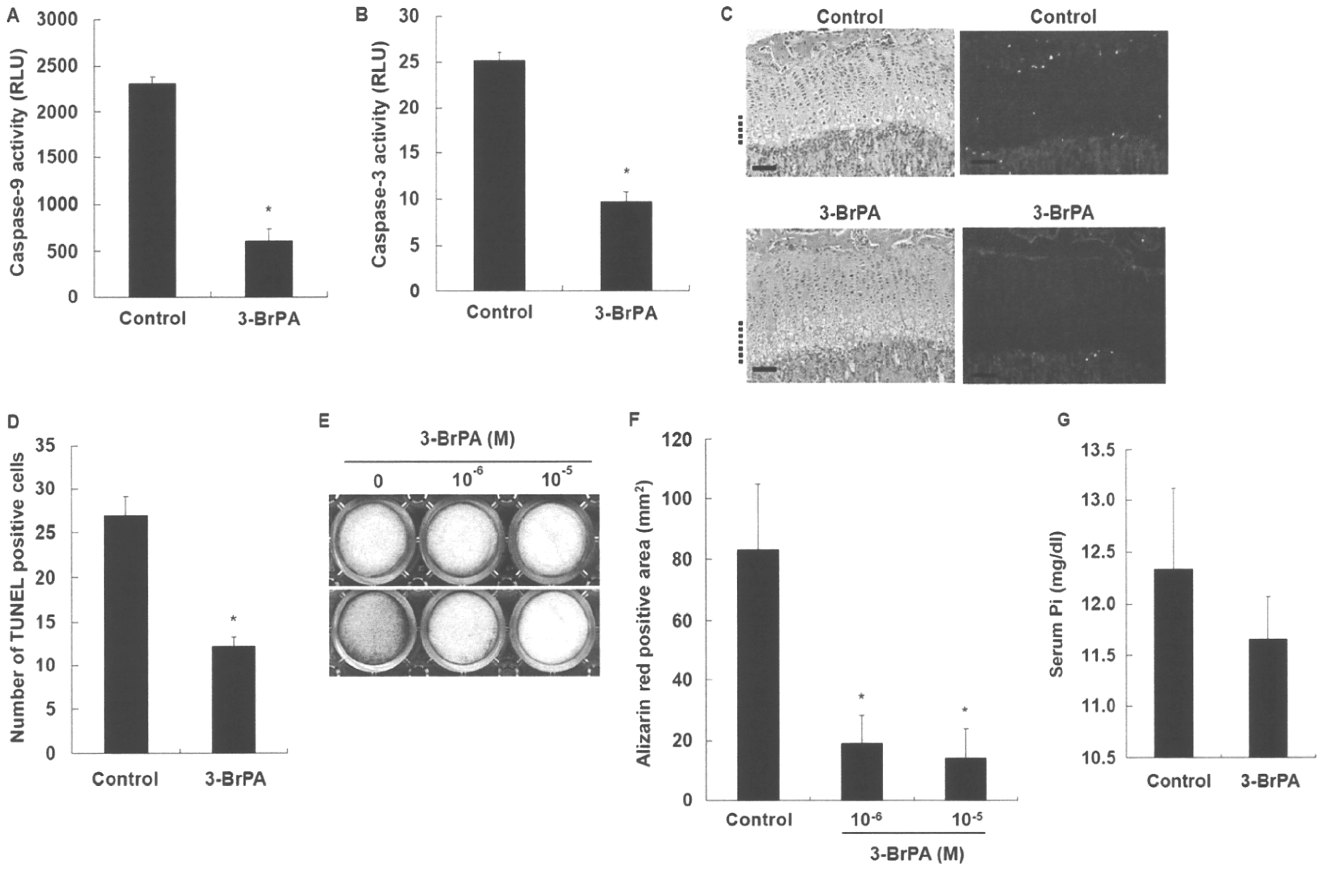

FIGURE 7. **Effects of 3-BrPA on chondrocyte apoptosis and calcification.** *A*, effects of 3-BrPA on caspase-9 activity. *B*, effects of 3-BrPA on caspase-3 activity. Cells were treated with 10^{-6} M 3-BrPA for 7 days and measured for caspase activity. *C*, histological examination of chondrocyte apoptosis. Hematoxylin/eosin staining (*left*) and TUNEL staining (*right*) were performed on tibial sections from 31-day-old control and 3-BrPA-treated mice. The hypertrophic zone is marked with *dotted lines*, and the *scale bars* indicate 200 μm. *D*, number of TUNEL-positive cells in tibial growth plates of control and 3-BrPA-treated mice. *E*, histochemical staining of chondrocytes. Cells were cultured for 7 days in the presence of 10^{-6} and 10^{-5} M 3-BrPA, and stained with Alcian blue for GAG synthesis (*upper*) and alizarin red S for mineralization (*lower*). *F*, quantification of alizarin red staining. *G*, serum P_i levels. Results are expressed as the mean ± S.E. of four separate experiments. *, significantly different from control ($p < 0.05$). *RLU*, relative light units.

pertrophic zone were most severe in *Hyp* mice compared with PFA- or 3-BrPA-treated mice, despite the fact that the number of TUNEL-positive cells are comparable in these mice. We postulate that the disorders in *Hyp* mice are congenital and irreversible and thus most severe, whereas the disorders seen in PFA- and 3-BrPA-treated mice are due to transient exposure of these agents and reversible and thus less severe.

Consistent with these *in vivo* results, *Hyp* chondrocytes in culture exhibited decreased activity of apoptotic signaling, including caspase-9 and caspase-3, apoptosis, and mineralization following reduced P_i uptake and cellular ATP synthesis. Furthermore, PFA or 3-BrPA diminished caspase-9 and caspase-3 activity, apoptosis, and mineralization in conjunction with a reduction in P_i uptake and ATP synthesis in WT chondrocytes. *Hyp* primary chondrocytes displayed a decrease in *Pit-1* (type III NPT) mRNA expression compared with WT chondrocytes, whereas there was no difference in type IIa NPT mRNA expression between WT and *Hyp* chondrocytes. WT and *Hyp* chondrocytes expressed no type I NPT mRNA. Meanwhile, GAG synthesis, which is an early event in chondrogenesis, was not reduced in *Hyp* chondrocytes, and PFA and 3-BrPA knockdown of *Pit-1* failed to decrease GAG synthesis in WT chondrocytes. *Pit-1* overexpression restored apoptosis and mineralization in *Hyp* chondrocytes. Taken together, these results suggest that P_i uptake via *Pit-1* and consequent ATP synthesis are critical in the regulation of late chondrogenesis, including apoptosis and mineralization. These results also suggest that the disruption of cellular P_i homeostasis causes abnormal endochondral ossification due to a reduction of ATP synthesis in Hyp mice. In support of our study, Zalutskaya *et al.* (32) have recently described that P_i activates mitochondrial apoptotic pathways and promotes endochondral ossification.

ATP Synthesis and Chondrogenesis—A notable and novel finding obtained in this study is that 3-BrPA inhibits apoptosis and mineralization in growth plate hypertrophic cartilage *in vivo* and primary chondrocytes *in vitro*. 3-BrPA is an alkylating agent that decreases cellular ATP via inhibition of hexokinase in glycolysis and has been shown to promote cancer cell death through activation of the mitochondrial pathway of apoptosis or necrosis (33). Of note, the ATP-depleting effect of 3-BrPA is prominent only in tumor cells but is not apparent in nontransformed cells (34). Hence, it has been proposed that 3-BrPA could be an anticancer agent for a variety of cancers. In addition to these effects on cancers, our results show that 3-BrPA inhibits the differentiation of cartilage, suggest-

ing that ATP generation is also necessary for nontransformed chondrocytes to differentiate and that chondrogenesis is thus an energy-dependent biological event.

Decreased Pit-1 Expression and Hyp Skeletal Phenotype—Decreased P_i uptake in *Hyp* chondrocytes is likely primarily due to reduced *Pit-1* mRNA expression. Type IIa NPT expression was not diminished in *Hyp* chondrocytes, and type I NPT was not expressed in chondrocytes. Earlier reports described that disturbed endochondral ossification was not rescued by P_i supplementation in *Hyp* mice (35–37), suggesting that intrinsic factors are involved. Miao *et al.* (5) showed that reduced expression of *PHEX* and MMP-9 is associated with cartilage abnormalities in *Hyp* mice. Our results suggest that *Pit-1* is one of these intrinsic factors responsible for the abnormal chondrogenesis seen in *Hyp* mice as well.

Regulation of Pit-1 Expression—The mechanism underlying down-regulation of *Pit-1* expression in *Hyp* chondrocytes is unknown. Recent studies have reported that stanniocalcin (STC) 1 increases *Pit-1* mRNA expression in osteoblasts (38), and STC1 and STC2 have been shown to regulate P_i uptake in chicken chondrocytes (39). STC1 stimulates renal P_i uptake and increases *Pit-1* expression in osteoblasts (40), whereas STC2 inhibits *Pit-1* expression and renal P_i uptake (38). Thus, STC1 and STC2 have an opposite action in the regulation of *Pit-1* expression. Therefore, it is intriguing to examine whether STC1 or STC2 is involved in *Pit-1* expression in chondrocytes. In preliminary experiments, we determined the expression of STC1 and STC2 mRNAs in WT and *Hyp* chondrocytes using RT-PCR and real-time PCR. The STC2 mRNA was expressed in both WT and *Hyp* chondrocytes at the same level (data not shown). However, the expression of STC1 mRNA was decreased in *Hyp* chondrocytes compared with WT chondrocytes (data not shown). These results suggest that STC1, but not STC2, regulates *Pit-1* expression in chondrocytes.

Involvement of FGF23—FGF23 (fibroblast growth factor 23) is a hormone that regulates serum P_i levels (41). FGF23 requires Klotho for its signaling as the coreceptor in addition to the canonical FGFR1(IIIc) (42, 43). Mice transgenic for FGF23 display a reduction in *Npt2a* expression in the renal proximal tubules (44), indicating that FGF23 is a negative regulator of *Npt2a* expression, raising the possibility that Klotho-dependent FGF23 signaling regulates *Pit-1* expression in chondrocytes as well. FGF23 expression is localized predominantly in osteoblasts, cementoblasts, and odontoblasts, with a sporadic expression in some chondrocytes, osteocytes, and cementocytes (45). However, we were not able to demonstrate FGF23 expression in primary mouse chondrocytes by RT-PCR. Further studies are needed to elucidate the relationship between FGF23 signaling and *Pit-1* expression in cartilage.

In conclusion, we have found in this study that chondrogenesis is modulated by cellular P_i uptake via *Pit-1* and cellular ATP synthesis and thus is a biological event that depends on mitochondrial energy generation. We believe that these findings should provide us with a novel concept and alternative approaches to study the cellular differentiation that occurs in physiological conditions and also to analyze the skeletal abnormalities seen in congenital hypophosphatemic disorders such as XLH.

Acknowledgments—We thank Drs. Kenichi Miyamoto and Hiroko Segawa (University of Tokushima Graduate School, Tokushima, Japan) for the kind gift of mouse Pit-1 cDNA.

REFERENCES

1. Zuscik, M. J., Hilton, M. J., Zhang, X., Chen, D., and O'Keefe, R. J. (2008) *J. Clin. Invest.* **118,** 429–438
2. Winters, R. W., Graham, J. B., Williams, T. F., McFalls, V. W., and Burnett, C. H. (1958) *Medicine* **37,** 97–142
3. Holm, I. A., Huang, X., and Kunkel, L. M. (1997) *Am. J. Hum. Genet.* **60,** 790–797
4. Eicher, E. M., Southard, J. L., Scriver, C. R., and Glorieux, F. H. (1976) *Proc. Natl. Acad. Sci. U.S.A.* **73,** 4667–4671
5. Miao, D., Bai, X., Panda, D. K., Karaplis, A. C., Goltzman, D., and McKee, M. D. (2004) *Bone* **34,** 638–647
6. Hayashibara, T., Hiraga, T., Sugita, A., Wang, L., Hata, K., Ooshima, T., and Yoneda, T. (2007) *J. Bone Miner. Res.* **22,** 1743–1751
7. Boyde, A., and Shapiro, I. M. (1980) *Histochemistry* **69,** 85–94
8. Kakuta, S., Golub, E. E., and Shapiro, I. M. (1985) *Calcif. Tissue Int.* **37,** 293–299
9. Mwale, F., Tchetina, E., Wu, C. W., and Poole, A. R. (2002) *J. Bone Miner. Res.* **17,** 275–283
10. Shapiro, I. M., and Boyde, A. (1984) *Metab. Bone Dis. Relat. Res.* **5,** 317–326
11. Virkki, L. V., Biber, J., Murer, H., and Forster, I. C. (2007) *Am. J. Physiol. Renal. Physiol.* **293,** F643–F654
12. Palmer, G., Zhao, J., Bonjour, J., Hofstetter, W., and Caverzasio, J. (1999) *Bone* **24,** 1–7
13. Mansfield, K., Teixeira, C. C., Adams, C. S., and Shapiro, I. M. (2001) *Bone* **28,** 1–8
14. Cecil, D. L., Rose, D. M., Terkeltaub, R., and Liu-Bryan, R. (2005) *Arthritis Rheum.* **52,** 144–154
15. Fujita, T., Meguro, T., Izumo, N., Yasutomi, C., Fukuyama, R., Nakamuta, H., and Koida, M. (2001) *Jpn. J. Pharmacol.* **85,** 278–281
16. Guicheux, J., Palmer, G., Shukunami, C., Hiraki, Y., Bonjour, J. P., and Caverzasio, J. (2000) *Bone* **27,** 69–74
17. Montessuit, C., Caverzasio, J., and Bonjour, J. P. (1991) *J. Biol. Chem.* **266,** 17791–17797
18. Wang, D., Canaff, L., Davidson, D., Corluka, A., Liu, H., Hendy, G. N., and Henderson, J. E. (2001) *J. Biol. Chem.* **276,** 33995–34005
19. Wu, L. N., Guo, Y., Genge, B. R., Ishikawa, Y., and Wuthier, R. E. (2002) *J. Cell. Biochem.* **86,** 475–489
20. Magne, D., Bluteau, G., Faucheux, C., Palmer, G., Vignes-Colombeix, C., Pilet, P., Rouillon, T., Caverzasio, J., Weiss, P., Daculsi, G., and Guicheux, J. (2003) *J. Bone Miner. Res.* **18,** 1430–1442
21. Shimomura, Y., Yoneda, T., and Suzuki, F. (1975) *Calcif. Tissue Res.* **19,** 179–187
22. Rowe, P. S., Ong, A. C., Cockerill, F. J., Goulding, J. N., and Hewison, M. (1996) *Bone* **18,** 159–169
23. Loghman-Adham, M. (1996) *Gen. Pharmacol.* **27,** 305–312
24. Swenson, C. L., Weisbrode, S. E., Nagode, L. A., Hayes, K. A., Steinmeyer, C. L., and Mathes, L. E. (1991) *Calcif. Tissue Int.* **48,** 353–361
25. Geschwind, J. F., Ko, Y. H., Torbenson, M. S., Magee, C., and Pedersen, P. L. (2002) *Cancer Res.* **62,** 3909–3913
26. Jones, A. R., Gillan, L., and Milmlow, D. (1995) *Contraception* **52,** 317–320
27. Ko, Y. H., Smith, B. L., Wang, Y., Pomper, M. G., Rini, D. A., Torbenson, M. S., Hullihen, J., and Pedersen, P. L. (2004) *Biochem. Biophys. Res. Commun.* **324,** 269–275
28. Gibson, G. (1998) *Microsc. Res. Tech.* **43,** 191–204
29. Eguchi, Y., Srinivasan, A., Tomaselli, K. J., Shimizu, S., and Tsujimoto, Y. (1999) *Cancer Res.* **59,** 2174–2181
30. Li, P., Nijhawan, D., Budihardjo, I., Srinivasula, S. M., Ahmad, M., Al-

nemri, E. S., and Wang, X. (1997) *Cell* **91,** 479–489
31. Rao, N. N., Gómez-García, M. R., and Kornberg, A. (2009) *Annu. Rev. Biochem.* **78,** 605–647
32. Zalutskaya, A. A., Cox, M. K., and Demay, M. B. (2009) *J. Cell. Biochem.* **108,** 668–674
33. Pelicano, H., Martin, D. S., Xu, R. H., and Huang, P. (2006) *Oncogene* **25,** 4633–4646
34. Xu, R. H., Pelicano, H., Zhou, Y., Carew, J. S., Feng, L., Bhalla, K. N., Keating, M. J., and Huang, P. (2005) *Cancer Res.* **65,** 613–621
35. Ecarot, B., Glorieux, F. H., Desbarats, M., Travers, R., and Labelle, L. (1992) *J. Bone Miner. Res.* **7,** 523–530
36. Tanaka, H., Seino, Y., Shima, M., Yamaoka, K., Yabuuchi, H., Yoshikawa, H., Masuhara, K., Takaoka, K., and Ono, K. (1988) *Bone Miner.* **4,** 237–246
37. Yoshikawa, H., Masuhara, K., Takaoka, K., Ono, K., Tanaka, H., and Seino, Y. (1985) *Bone* **6,** 235–239
38. Yoshiko, Y., Candeliere, G. A., Maéda, N., and Aubin, J. E. (2007) *Mol. Cell. Biol.* **27,** 4465–4474
39. Wu, S., Yoshiko, Y., and De Luca, F. (2006) *J. Biol. Chem.* **281,** 5120–5127
40. Ishibashi, K., and Imai, M. (2002) *Am. J. Physiol. Renal Physiol.* **282,** F367–F375
41. Fukumoto, S., and Yamashita, T. (2007) *Bone* **40,** 1190–1195
42. Kurosu, H., Ogawa, Y., Miyoshi, M., Yamamoto, M., Nandi, A., Rosenblatt, K. P., Baum, M. G., Schiavi, S., Hu, M. C., Moe, O. W., and Kuro-o, M. (2006) *J. Biol. Chem.* **281,** 6120–6123
43. Urakawa, I., Yamazaki, Y., Shimada, T., Iijima, K., Hasegawa, H., Okawa, K., Fujita, T., Fukumoto, S., and Yamashita, T. (2006) *Nature* **444,** 770–774
44. Shimada, T., Urakawa, I., Yamazaki, Y., Hasegawa, H., Hino, R., Yoneya, T., Takeuchi, Y., Fujita, T., Fukumoto, S., and Yamashita, T. (2004) *Biochem. Biophys. Res. Commun.* **314,** 409–414
45. Yoshiko, Y., Wang, H., Minamizaki, T., Ijuin, C., Yamamoto, R., Suemune, S., Kozai, K., Tanne, K., Aubin, J. E., and Maeda, N. (2007) *Bone* **40,** 1565–1573

Journal of Human Genetics (2011), 1–3

www.nature.com/jhg

COMMENTARY

Hypophosphatasia now draws more attention of both clinicians and researchers: A Commentary on prevelance of c. 1559delT in *ALPL*, a common mutation resulting in the perinatal (lethal) form of hypophosphatasias in Japanese and effects of the mutation on heterozygous carriers

Keiichi Ozono and Toshimi Michigami

Journal of Human Genetics advance online publication, 10 February 2011; doi:10.1038/jhg.2011.6

Hypophosphatsia is a skeletal disease due to an inborn error of metabolism characterized by deficient activity of the tissue-nonspecific alkaline phosphatase.[1,2] Alkaline phosphatase (ALP) is a membrane-bound metalloenzyme that consists of a group of isoenzymes encoded by four different gene loci: tissue-nonspecific, intestinal, placental and germ-cell ALP. Tissue-nonspecific alkaline phosphatase is expressed in almost all cells and three organs, liver, bone and kidney, have high activity of ALP. Thus, tissue-nonspecific alkaline phosphatase is also called ALP liver/bone/kidney (ALPL). The mouse counter part is called Akp2. Tissue-nonspecific alkaline phosphatase hydrolyzes inorganic pyrophosphate, an inhibitor of mineralization, and increases the local concentration of inorganic phosphate. Therefore, hypomineralization of skeleton and rachitic change of bone is associated with hypophosphatasia.

Hypophosphatasia is highly variable in its clinical expression. On the basis of the age of manifestation and its severity, hypophosphatasia is divided into six subtypes (Table 1). The most severe form of hypophosphatasia is a perinatal form, which is also called a lethal form. This form presents clinically either before or in the newborn period. The patients with this form exhibit severe defect of bone mineralization including craniotabes, bone deformity, short stature and narrow chest, and suffer from respiratory failure (Figure 1). However, some patients of this form can survive because of advances in neonatology.[3] Recently, non-lethal benign form of perinatal hypophosphatasia has been recognized, which is associated with no apparent defects of mineralization.[4,5] An infantile form is characterized by infantile onset and often associated with poor weight gain, hypercalcemia and respiratory difficulties. This form shows still rather high mortality. A childhood form is manifested at the age of 2 or 3 with premature loss of teeth, rachtic change of long bones and mild short stature. An adult form is sometimes associated with pathologic bone fracture and an odonto types means a form of only teeth manifestation. Diagnosis of hypophosphatasia is made on the basis of the clinical features, skeletal X-ray findings and low activity of ALP associated with elevation of its substrate, such as phosphoethanolamine, inorganic pyrophosphate and pyridoxal-5′-phosphate. We described diagnostic criteria of hypophosphatasia proposed by the Japanese Hypophosphatasia Study Group at http://www.bone.med.osaka-u.ac.jp/english/b5/.

Hypophosphatasia is usually inherited in an autosomal recessive manner, but can be expressed in an autosomal dominant manner in milder forms.[6] The *ALPL* gene is located on the short arm of chromosome 1 (1p36.1–p34), and contains 12 exons. The product consists of 507 amino acids including residues of the signal peptide. Hypophosphatasia is caused by various mutations in the *ALPL* gene. Currently, more than 200 mutations of the *ALPL* gene in patients with hypophosphatasia have been registered in the *ALPL* gene mutations database (http://www.sesep.uvsq.fr/Database.html). Most mutations described to date are missense mutations (80%), and the remainder was several deletion and insertion mutations of one to four nucleotides. Large deletions of the gene are rare (1.3%). Correlations of genotype and phenotype have been reported on the basis of clinical data of the patients with hypophosphatasia, enzymatic activity and computer-assisted modeling.[2]

We previously reported that the most and the second-most frequent mutations in Japanese patients are T1559del and F310L, respectively.[5] These mutations are renamed to c.1559delT and p.F327 L, respectively, based on the recent standardized nomenclature. Interestingly, both mutations are unique to Japanese. The common mutations, c.1559delT and p.F327 L, are associated with lethal and the perinatal non-lethal forms of hypophosphatasia, respectively. This is an example of

Professor K Ozono is at the Department of Pediatrics, Osaka University Graduate School of Medicine, 2-2 Yamadaoka, Suita, Osaka 565-0871, Japan and T Michigami is at the Department of Bone and Mineral Research Osaka Medical Center and Research Institute for Maternal and Child Health, 840 Murodo-cho, Izumi, Osaka 594-1101, Japan.
E-mail: keioz@ped.med.osaka-u.ac.jp